



저작자표시-비영리-변경금지 2.0 대한민국

이용자는 아래의 조건을 따르는 경우에 한하여 자유롭게

- 이 저작물을 복제, 배포, 전송, 전시, 공연 및 방송할 수 있습니다.

다음과 같은 조건을 따라야 합니다:



저작자표시. 귀하는 원저작자를 표시하여야 합니다.



비영리. 귀하는 이 저작물을 영리 목적으로 이용할 수 없습니다.



변경금지. 귀하는 이 저작물을 개작, 변형 또는 가공할 수 없습니다.

- 귀하는, 이 저작물의 재이용이나 배포의 경우, 이 저작물에 적용된 이용허락조건을 명확하게 나타내어야 합니다.
- 저작권자로부터 별도의 허가를 받으면 이러한 조건들은 적용되지 않습니다.

저작권법에 따른 이용자의 권리는 위의 내용에 의하여 영향을 받지 않습니다.

이것은 [이용허락규약\(Legal Code\)](#)을 이해하기 쉽게 요약한 것입니다.

[Disclaimer](#)

A Doctoral Dissertation

**A study on the regulation of neuronal
cell death through mitochondrial
calcium and membrane potential**

Jin-Ji Wu

Department of Medicine

Graduated School

Jeju National University

August, 2013

미토콘드리아 칼슘과 막전압을 통한 신경세포 손상사멸의 조절에 관한 연구


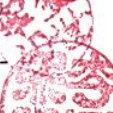



지도교수: 은 수 용

오 금 희

이 논문을 의학 박사학위 논문으로 제출함

2013년 8월

오금희의 의학 박사학위 논문을 인준함

| | | | | |
|-------|---|---|---|---|
| 심사위원장 | 정 | 성 | 철 |  |
| 위 | 원 | 김 | 재 |  |
| 위 | 원 | 이 | 희 |  |
| 위 | 원 | 박 | 민 |  |
| 위 | 원 | 은 | 수 |  |

제주대학교 대학원

2013년 8

**A study on the regulation of neuronal cell death through
mitochondrial calcium and membrane potential**

Jin-Ji Wu

(Supervised by professor **Su-Yong Eun**)

**A thesis submitted in partial fulfillment of the requirement for the
degree of doctor of philosophy in medicine**

August, 2013

This thesis has been examined and approved.

Sung Chert Jung

Se Gae Kim

Sung Hee Lee

Soo Min Park

Su Yong Eun

2013.6.13

Date

Department of Medicine

Graduated School

Jeju National University

ABSTRACT

It has been demonstrated that even a small mitochondrial depolarization is sufficient to prevent neuronal cell death by suppressing mitochondrial calcium overload since mitochondrial membrane potential ($\Delta\Psi_m$) contributes to determining a driving force for calcium to enter the mitochondria. Therefore, mitochondrial depolarization has been recently evaluated as a novel mechanism of neuroprotection via inhibiting neurotoxic mitochondrial calcium overload during neuronal insults. The active compounds from the peel of *citrus* fruits are known to exert significant biological activities including anti-inflammatory and anti-oxidant properties. A growing body of evidence has recently demonstrated that these compounds recover damaged cognitive function in the models of neurodegenerative disease. However, the specific mechanism of neuroprotective effects has not to be clearly elucidated yet. Therefore, we investigated the neuroprotective mechanism of *citrus* peel extracts (CPE) against oxidative neurotoxicity implicated in neurodegenerative diseases. The results showed that neuronal viability was significantly increased by CPE in H₂O₂-treated neuronal HT-22 cells, which were used as an *in vitro* model of oxidative neurotoxicity. The CPE demonstrated a robust scavenging activity of intracellular reactive oxygen species (ROS). CPE treatment significantly blocked H₂O₂-induced Ca²⁺ overload in both the cytosol and the mitochondria as indicated by Fluo-4 and Rhod-2 respectively, and inhibited neuronal apoptosis cascades including caspase 3. Additionally, we determined using TMRM and JC-1 fluorometric probes for mitochondrial membrane potential ($\Delta\Psi_m$) that the CPE and CPE compounds such as nobiletin are capable of inducing a mild mitochondrial depolarization which has been recently evaluated as a novel mechanism of neuroprotection via inhibiting mitochondrial Ca²⁺ overload during neuronal insults. Our findings suggest a dual neuroprotective mechanism of CPE via not only anti-oxidant activity but also $\Delta\Psi_m$ regulation.

In the next study, we investigated the exact neuroprotective mechanism of mitochondrial membrane depolarization in neuronal insults-induced cell death, separated from anti-oxidant mechanism. For this experimental aim, we tested the neuroprotective mechanism of indomethacin, non-steroid anti-inflammatory drugs (NSAIDs), which does not have antioxidant activity but evokes mitochondrial membrane depolarization. The results demonstrated that neuronal viability was significantly increased by indomethacin treatment in glutamate-exposed primary cortical neurons as a glutamate-induced neurotoxicity model. This neuroprotective effect was abolished by 5-hydroxydecanoate (5HD), a ATP-sensitive K^+ channels (mitoK_{ATP}) channel blocker. This blockade of mitoK_{ATP} channels by 5HD treatment significantly inhibited indomethacin-induced mitochondrial depolarization and also abolished indomethacin-induced inhibitory effect on mitochondrial calcium overload. It also suppressed mitochondrial dysfunction-associated parameters such as ROS generation and mitochondrial permeability transition pore (mPTP) open.

Taken together, these results suggest that the active compounds of CPE and indomethacin may be considered as promising neuroprotective agents via inducing a mitochondrial depolarization. In addition, we propose here that mitochondrial ion channels and transporters such as mitoK_{ATP} channels could be evaluated as the novel therapeutic targets for neuroprotection against neuronal cell death implicated in one of the critical causes of brain ischemia and neurodegenerative diseases.

Keywords: mitochondrial calcium, mitochondrial membrane potential, calcium, mitochondria, Indomethacin, *Citrus*

CONTENTS

| | |
|---------------------------------------|-----------|
| ABSTRACT | 1 |
| CONTENTS..... | 3 |
| LIST OF FIGURES AND TABLE..... | 4 |
| PART I | 6 |
| PART II..... | 8 |
| REFERENCE..... | 67 |
| ABSTRACT IN KOREAN | 73 |

LIST OF FIGURES AND TABLE

| | |
|--|----|
| Fig.1. Neuroprotective effects of CPE against H ₂ O ₂ -induced oxidative neurotoxicity | 22 |
| Fig.2. Effect of CPE on procaspase-3 and PARP against H ₂ O ₂ -induced oxidative neurotoxicity..... | 23 |
| Fig.3. Anti-oxidant activities of CPE..... | 24 |
| Fig.4. CPE evokes a mild mitochondrial depolarization, as indicated in real-time measurement of $\Delta\Psi_m$ | 27 |
| Fig.5. Differential effects of single compounds of CPE on JC-1 F _{red} /F _{green} ratio indicative of $\Delta\Psi_m$ | 32 |
| Fig.6. Inhibitory effects of CPE on H ₂ O ₂ -induced cytosol calcium overload..... | 34 |
| Fig.7. Inhibitory effects of CPE on H ₂ O ₂ -induced mitochondrial calcium overload..... | 36 |
| Fig.8. Neuronal purity in primary cortical neuron cultures..... | 50 |
| Fig.9. Effects of indomethacin and 5HD on glutamate-induced neuronal toxicity..... | 51 |

| | |
|---|----|
| Fig.10. Anti-oxidant activities of indomethacin..... | 52 |
| Fig.11. Effect of indomethacin on the mitochondrial membrane potential, cytosol calcium and mitochondrial calcium..... | 54 |
| Fig.12. Inhibitory effect of 5HD on indomethacin-induced mitochondrial depolarization..... | 58 |
| Fig.13. Effects of indomethacin and 5HD on glutamate-induced mitochondrial superoxide generation..... | 59 |
| Fig.14. Effects of indomethacin and 5HD on glutamate-induced mitochondrial mitochondrial calcium overload..... | 62 |
| Fig.15. Effects of indomethacin and 5HD on glutamate-induced mPTP opening..... | 64 |
| Table1. Flavonoids content (mg/g) contained in CPE..... | 30 |

PART I

| | |
|---|-----------|
| 1. INTRODUCTION..... | 11 |
| 2. MATERIALS AND METHODS..... | 13 |
| 2.1. Materials | |
| 2.2. Preparation of the extract and compound | |
| 2.3. Cell culture | |
| 2.4. Real-time measurement of mitochondrial membrane potential ($\Delta\Psi_m$) | |
| 2.5. Flow cytometric and imaging analyses of $\Delta\Psi_m$ | |
| 2.6. Flow cytometric analyses of cytosol and mitochondrial Ca^{2+} | |
| 2.7. Mitochondrial Ca^{2+} Imaging | |
| 2.8. Measurement of cell viability | |
| 2.9. Morphological analysis of apoptosis | |
| 2.10. Western blotting analysis | |
| 2.11. Measurement of intracellular reactive oxygen species (ROS) | |
| 2.12. DPPH free radical scavenging assay | |
| 2.13. Measurement of superoxide dismutase (SOD) activities | |
| 2.14. Measurement of catalase activities | |
| 2.15. Statistics analysis | |
| 3. RESULTS | 20 |
| 3.1. Neuroprotective effects of CPE against H_2O_2 -induced oxidative neurotoxicity | |

- 3.2. Antioxidant activities of CPE
- 3.3. Mild-depolarizing effects of CPE on $\Delta\Psi_m$
- 3.4. Differential effects of single compounds of CPE on $\Delta\Psi_m$
- 3.5. Inhibitory effects of CPE on H_2O_2 -induced overload of Ca^{2+} in both the cytosol and the mitochondria

4. DISCUSSION..... 37

PART II

1. INTRODUCTION..... 41

2. MATERIALS AND METHODS.....43

2.1. Materials

2.2. Cell culture

2.3. Immunofluorescence microscopy and labeling of mitochondria

2.4. Measurement of cell viability

2.5. Real-time measurement of $\Delta\Psi_m$

2.6. Dural recording of cytosolic and mitochondrial calcium

2.7. DPPH radical scavenging assay

2.8. Intracellular reactive oxygen species (ROS) measurement

2.9. Real-time measurement of mitochondrial superoxide generation

2.10. Mitochondrial permeability transition pore (mPTP) assay

2.11. Statistics analysis

3. RESULTS48

3.1. Purity of primary cortical neuron

3.2. Mitochondrial K_{ATP} channel blockade abolishes neuroprotective effect of indomethacin on glutamate-induced neurotoxicity in primary cortical neuron

3.3. Mitochondrial K_{ATP} channel blockade abolishes neuroprotective effect of indomethacin on glutamate-induced ROS generation

- 3.4. Effect of indomethacin on the mitochondrial membrane potential, cytosol calcium and mitochondrial calcium
- 3.5. Mitochondrial K_{ATP} channel blockade abolishes neuroprotective effect of indomethacin on mitochondrial membrane potential
- 3.6. Mitochondrial K_{ATP} channel blockade abolishes neuroprotective effect of indomethacin on glutamate-induced mitochondrial superoxide generation
- 3.7. Mitochondrial K_{ATP} channel blockade abolishes neuroprotective effect of indomethacin on glutamate-induced mitochondrial calcium overload
- 3.8. Mitochondrial K_{ATP} channel blockade abolishes neuroprotective effect of indomethacin on glutamate-induced mPTP opening

4. DISCUSSION.....65

PART I

**Dual neuroprotective mechanisms of
Citrus sunki Peel Extract against
neuronal oxidative stress**

1. Introduction

The electron transport chains maintain an electrochemical gradient of approximately -180 mV across the inner mitochondrial membrane (Kroemer *et al.*, 2007) (Hung *et al.*, 2010). Mitochondrial membrane potential ($\Delta\Psi_m$) contributes to determining a driving force for Ca^{2+} to enter the mitochondria via Ca^{2+} -permeable channels such as the mitochondrial Ca^{2+} uniporter (Kirichok *et al.*, 2004). Therefore, the entry of Ca^{2+} into the mitochondria is highly dependent on $\Delta\Psi_m$. It has been demonstrated that even a small mitochondrial depolarization is sufficient to prevent mitochondrial Ca^{2+} overload (Nunez *et al.*, 2006) (Valero *et al.*, 2008) and the subsequent apoptosis (Garcia-Martinez *et al.*, 2010). This partial depolarization of mitochondrial membrane should be fundamentally distinguished from $\Delta\Psi_m$ dissipation, which means a full-blown mitochondrial depolarization at the almost final stage in mitochondria-dependent apoptotic pathways.

The neuroprotective effects of the minocycline (Garcia-Martinez *et al.*, 2010), NSAIDs (Sanz-Blasco *et al.*, 2008), and KB-R7943 (Storozhevych *et al.*, 2010) against excitotoxic insults have recently been proposed to be attributable to their intrinsic ability to induce mild mitochondrial depolarization in resting neurons. Owing to a growing body of evidences, $\Delta\Psi_m$ is evaluated as a promising target to modulate mitochondrial Ca^{2+} overload which might be the triggering point of neuronal cell death. In this context, the compounds that are able to reduce the driving force for Ca^{2+} entry into the mitochondria by inducing a mild mitochondrial depolarization, may be considered as promising neuroprotective agents.

Natural extracts from fruits of the genus *Citrus* have been reported to harbor an abundance of flavonoids and to exert significant biological activities such as anti-inflammatory effects, anti-atherogenic effects and anti-cancer activity (Galati *et al.*, 1994) (Lee *et al.*, 2001) (Ko *et al.*, 2010). The majority of these flavonoids are localized in *Citrus* fruit peel, rather than in the flesh of the fruit. In particular, *Citrus* peel is a rich source of

flavonol glycosides (rutin, etc.), flavanone glycosides (hesperidin and naringin, etc.) and polymethoxylated flavones (nobiletin, tangeretin and sinensetin, etc.) which are quite rare in other plants (Choi *et al.*, 2007).

Recently, the neuroprotective activities of active compounds from *Citrus* peel extract have been demonstrated in several studies. Nobiletin, a polymethoxylated flavone isolated from *Citrus* fruits, has been shown to enhance damaged cognitive function in several animal models such as ischemia, learning and memory impairment, olfactory bulbectomy-induced, and transgenic Alzheimer's disease animal models (Onozuka *et al.*, 2008). We reported in the previous study that nobiletin suppresses excess microglia activation, which has been implicated in both neuroinflammation and neurodegeneration (Clapham, 2007). However, the cellular and molecular mechanisms underlying these neuroprotective effects of *Citrus* peel have not to be clearly elucidated yet.

In this study, the neuroprotective mechanism of ethanolic peel extract (CPE) of *Citrus sunki* Hort. ex Tanaka was investigated against H₂O₂-induced oxidative neurotoxicity model. Finally, we suggest a possible dual neuroprotective mechanisms of CPE in the present study. One of the dual mechanisms is associated with anti-oxidant activities of CPE via scavenging reactive oxygen species (ROS). And the other is associated with the partial blockade of mitochondrial Ca²⁺ uptake owing to the mild depolarization of the mitochondrial membrane.

2. Materials and methods

2.1. Materials

Dulbecco's Modified Eagle Medium (DMEM), fetal bovine serum (FBS), penicillin/streptomycin, 5,5',6,6'-tetrachloro-1,1',3,3'-tetraethylbenzimidazolcarbocyanineiodide (JC-1), tetramethylrhodamine methyl ester (TMRM), fluo-4 acetoxymethyl ester (Fluo-4 AM) and rhod-2 acetoxymethyl ester (Rhod-2 AM) were purchased from Invitrogen (Carlsbad, CA, USA). Anti-procaspase 3 and anti-poly (ADP-ribose) polymerase (PARP) were purchased from Santa Cruz Biotechnology (Santa Cruz, CA, USA), anti- β -actin from Cell Signaling Technology (Danvers, MA, USA) and horseradish peroxidase (HRP)-conjugated secondary antibodies from Vector Laboratories (Burlingame, MA, USA). All other reagents were purchased from Sigma-Aldrich (St Louis, MO, USA), unless indicated otherwise.

2.2. Preparation of the extract and compounds

CPE was prepared from the peel of *Citrus sunki* Hort. ex Tanaka, as described previously (Choi *et al.*, 2007). Briefly, the peels from mature fruits of *C. sunki* were obtained from Seogwipo-si on Jeju island, South Korea in September, 2008. The powered peels (10 g) were extracted twice for 72 h with 200 ml of ethanol-water (7:3, v/v) at room temperature. The extract was filtered, lyophilized and stored at -20 °C until use. High performance liquid chromatography (HPLC) analyses using a Waters 2695 Alliance HPLC system (Waters Corp., Milford, MA) showed that CPE contained abundant flavonoids, such as rutin (5.32 mg/g), hesperidin (14.15 mg/g), nobiletin (8.67 mg/g), tangeretin (14.52 mg/g), sinensetin (0.91 mg/g). Rutin, hesperidin, nobiletin and tangeretin were purchased from Sigma-Aldrich

(St Louis, MO, USA) to explore single compounds responsible for CPE effects on $\Delta\Psi_m$.

2.3. Cell culture

HT-22 neurons as an immortalized hippocampal neuronal cell line (Breyer *et al.*, 2007) (a generous gift from Dr. B.H. Lee, Gachon University of Medicine and Science, South Korea) were cultured in DMEM containing 10% FBS, and 1% penicillin/streptomycin, and maintained at 37°C in a humidified atmosphere of 5% CO₂.

2.4. Real-time measurement of mitochondrial membrane potential ($\Delta\Psi_m$)

TMRM is a cell-permeant, cationic fluorescent probe that is sequestered by mitochondria in proportion to $\Delta\Psi_m$ (Scaduto and Grotyohann, 1999). The cells on poly-L-lysine-coated cover glasses were loaded with 100 nM TMRM for 30 min, washed for three times and mounted on a recording chamber of an epifluorescence inverted microscope Olympus IX71 (Olympus, Japan). The cells were superfused with normal Tyrode solution by fast flow system using tubing. Normal Tyrode solution contained (mM): 140 NaCl, 0.5 MgCl₂, 1.8 CaCl₂, 5.4 KCl, 10 HEPES, 5 glucose. CPE application was accomplished by changing perfusion medium containing CPE. Digitized fluorescence images were acquired at 30 s intervals with a cooled-charge device (CCD) camera (Cascade, Roper Scientific, USA), and analyzed in a personal computer using Metafluor software (Universal Imaging, Sunnyvale, CA, USA).

2.5. Flow cytometric and imaging analyses of $\Delta\Psi_m$

$\Delta\Psi_m$ was also determined by the membrane potential-sensitive ratiometric dye JC-1 in accordance with the manufacturer's recommended protocols (Salvioli *et al.*, 1997). After CPE

treatment, the cells were loaded with JC-1 (5 μ M) for 30 min, washed 3 times and immediately analyzed with a flow cytometer (Becton Dickinson, USA) or imaged on a confocal laser scanning microscope (FV500, Olympus, Japan). Carbonyl cyanide *m*-chlorophenylhydrazone (CCCP, 10 μ M) was used as a mitochondrial uncoupler to induce total mitochondrial membrane depolarization which mimics apoptotic total $\Delta\Psi_m$ dissipation shown at the almost final stage in mitochondria-dependent apoptotic pathway.

JC-1 is a cell-permeant, cationic fluorescent probe which exhibits $\Delta\Psi_m$ -dependent accumulation in the mitochondria, the membrane potential of which is extremely hyperpolarized to approximately -180 mV. The more depolarized the mitochondrial membrane becomes, the fewer JC-1 molecules are accumulated in the mitochondria. Therefore, mitochondrial membrane depolarization decreases the ratio of JC-1 aggregates to JC-1 monomers. This is indicated by a decrease in the ratio of red to green fluorescence intensity ($F_{\text{red}}/F_{\text{green}}$ ratio) since red fluorescence emissions (~590 nm) are obtained from JC-1 aggregates and green fluorescence emissions (~525 nm) are generated by JC-1 monomers.

2.6. Flow cytometric analyses of cytosol and mitochondrial Ca^{2+}

For the measurement of cytosolic and mitochondrial Ca^{2+} levels, cell-permeable Fluo-4 AM and Rhod-2 AM are used as the selective Ca^{2+} indicators respectively. Fluorescence intensities of them increase upon Ca^{2+} binding (>100-fold). As cationic Rhod-2 AM shows potential-driven uptake into the mitochondria, it has been used as a selective indicator for mitochondrial Ca^{2+} . After CPE treatment, the cells were loaded with 2 μ M Fluo-4 AM and 2 μ M Rhod-2 AM respectively for 30 min, washed 3 times. The fluorescence intensities were immediately analyzed with a flow cytometer (Becton Dickinson, USA).

2.7. Mitochondrial Ca²⁺ Imaging

For Rhod-2 confocal microscopic imaging, the cells were seeded on poly-L-lysine coated cover glasses. After CPE treatment, the cells were loaded with Rhod-2 AM (5 μ M) for 2 h at 4°C, washed 3 times and transferred to 37°C for an additional 2 h. After fixing and mounting, Rhod-2 fluorescence was imaged on a confocal laser scanning microscope (FV500, Olympus, Japan) using a cooled charge-coupled device (CCD) camera controlled by Flow View 4.2 software (Olympus, Japan).

2.8. Measurement of cell viability

MTT [3-(4,5-dimethylthiazol-2-yl)-2,5-diphenyl tetrazolium bromide] was used to evaluate the effects of CPE on cell viability, as described previously (Cui *et al.*, 2010). In brief, after CPE treatment, 200 μ l MTT (2 mg/ml) was added to each well in 24-well plates and incubated for an additional 2 hours. The liquid in each well was then aspirated and 500 μ l dimethyl sulfoxide (DMSO) was added, and then absorbance was read with a microplate reader (Sunrise, Tecan, Austria).

2.9. Morphological analysis of apoptosis

The degree of apoptosis was determined by nuclear staining with Hoechst 33342, a cell-permeant DNA-specific fluorescent dye. Cells were placed in 24-well plates, treated, and incubated for 10 min with Hoechst 33342 (5 μ g/ml). Nuclear chromatin condensation was then observed under a IX-71 fluorescent microscope (Olympus, Japan) equipped with a CoolSNAP-Pro color digital camera (Media Cybernetics, Silver Spring, MD, USA).

2.10. Western blotting analysis

Cells were washed once with phosphate-buffered saline (PBS; pH 7.4) and lysed with modified RIPA buffer (10 mM Tris-HCl; pH 7.4, 150 mM NaCl, 1 mM EGTA, 0.1% SDS, 1 mM NaF, 1 mM Na₃VO₄, 1 mM PMSF, 1 µg/ml aprotinin, and 1 µg/ml leupeptin). Protein (50 µg) was separated by sodium dodecyl sulfate-polyacrylamide gel electrophoresis (SDS-PAGE) and then electro-transferred onto a polyvinylidene fluoride (PVDF) membrane (BIO-RAD, CA, USA) using Towbin transfer buffer (192 mM glycine, 25 mM Tris, and 20% methanol; pH 8.3). The blots were incubated with 5% skim milk in TTBS (25 mM Tris, 150 mM NaCl, PH 7.4, containing 0.1% Tween 20) for 2 h at room temperature to block nonspecific binding. Subsequently, the membranes were incubated overnight at 4°C with anti-procaspase 3 (1:1000), anti-PARP (1:1000) and anti- β -actin antibody (1:5000). The blots were washed 3 times with TTBS and incubated with the appropriate horseradish peroxidase (HRP)-conjugated secondary antibodies (1:5000) for 1 h at room temperature. After several washes, the blots were developed using enhanced chemiluminescence detection reagents (Intron Biotechnology, South Korea) according to the manufacturer's instructions. Optical densities of the band were quantified with an Image J analyzer (<http://rsb.info.nih.gov/ij/>) and normalized with those of β -actin.

2.11. Measurement of intracellular reactive oxygen species (ROS)

The cells were seeded on 96-well tissue culture plates at 2×10^4 cells/well and pretreated for 30 min with CPE followed by 1 mM H₂O₂ for an additional 30 min. After the addition of 50 µM of DCF-DA (2',7'-dichlorodihydrofluorescein diacetate), fluorometric analysis was conducted at an excitation/emission wavelength of 485 nm/535 nm using a microplate reader (Spectra Fluor, Tecan, Austria).

2.12. DPPH free radical scavenging assay

Various concentrations of CPE (10 μ l) were added to 190 μ l (0.15 mM in ethanol) of DPPH (1,1-diphenyl-2-picrylhydrazyl radical) and vigorously mixed. The mixture was incubated for 1 h in darkness at room temperature, and the absorbance was read at 517 nm using a microplate reader (Sunrise, Tecan, Austria). The percentage level of DPPH scavenging was calculated according to the following formula: % Radical Scavenging = $[(A - A_s)/A] \times 100$, in which A is the absorbance of DPPH and A_s is its absorbance after citrus peel extract treatment.

2.13. Measurement of superoxide dismutase (SOD) activities

The cells were scraped and suspended in 10 mM phosphate buffer (pH 7.5) after treatment and then lysed via sonication. The lysates were incubated on ice for an additional 10 min in 1% Triton X-100 and centrifuged for 30 min at 5,000 \times g at 4°C. The protein content of the supernatant was determined by the Bradford method. Total SOD activity was evaluated by measuring the inhibition rate of epinephrine auto-oxidation (Misra and Fridovich, 1972). Fifty micrograms of protein were added to 50 mM phosphate buffer (pH 10.2) containing 1mM epinephrine. Epinephrine rapidly undergoes auto-oxidation to generate adrenochrome, a pink-colored product, which was analyzed at 480 nm with a UV-visible spectrophotometer (Shimadzu, Germany) in kinetic mode. The SOD activities were expressed in units/ mg protein.

2.14. Measurement of catalase activities

Cellular protein was prepared via the method described above (See *Measurement of*

superoxide dismutase (SOD) activities). Fifty micrograms of protein were added to 50 mM phosphate buffer (pH 7.0) containing 100 mM H₂O₂ and subsequently incubated for 2 min at 37°C, after which the absorbance was monitored for 2 min at 240 nm. The change in absorbance was proportional to the breakdown of H₂O₂. Catalase activities were expressed in terms of units/ mg protein.

2.15. Statistics analysis

Data are expressed as mean value \pm standard error of the mean (SEM) of three or four samples in one independent experiment. Statistical analyses were conducted using Student's *t*-test. The differences between groups were regarded as statistically significant when $p < 0.05$.

3. Results

3.1. Neuroprotective effects of CPE against H₂O₂-induced oxidative neurotoxicity

The neuroprotective effects of CPE against H₂O₂-induced oxidative neurotoxicity were evaluated via MTT assays (Fig. 1-A). HT-22 neurons were treated with H₂O₂ (1mM) for 12 h in the presence or absence of CPE. Pretreatment with various concentrations (50, 100 and 200 µg/ml) of CPE was carried out for 1 h prior to H₂O₂ stimulation. The CPE treatments markedly increased cell viability against H₂O₂-induced oxidative neurotoxicity in a dose-dependent manner, by 34.8±3.8%, 43.9±7.9% and 46±10.0% respectively, relative to the group treated with H₂O₂ alone. The CPE alone evidenced no cytotoxicity at concentrations below 200 µg/ml. The cell viability was slightly decreased in case of 400 µg/ml of CPE alone in lactate dehydrogenase (LDH) release assays or MTT assays (data not shown).

The degree of apoptosis was determined by nuclear staining with Hoechst 33342, a cell-permeant DNA-specific fluorescent dye (Fig. 1-B). The H₂O₂-treated cells demonstrated significant chromatin condensation, which is indicative of apoptosis. However, CPE (200 µg/ml) also markedly reduced H₂O₂-induced chromatin condensation, which is consistent with the cell viability data shown in Fig. 1-A.

Generally, ROS induces mitochondrial dysfunction and the subsequent opening of the mitochondrial permeability transition pore (mPTP). Mitochondrial cytochrome C is then released into cytoplasm through the mPTP, which evokes the activation of caspase 3. This protease, in turn, degrades several proteins including PARP, an important DNA repair enzyme. Regarding these apoptotic cascades, the results of Western blotting analyses demonstrated H₂O₂-induced reductions of procaspase-3 (Fig. 2-A) and poly PARP (Fig. 2-B), which are associated with caspase 3 activation and PARP cleavage. They were almost fully recovered by 64.9±5.9% and 52.2±11.3%, respectively in the CPE (200 µg/ml)-treated cells.

These results demonstrate that CPE exerts neuroprotective effects against H₂O₂-induced oxidative neurotoxicity.

3.2. Antioxidant activities of CPE

We investigated the antioxidant activities of CPE against H₂O₂-treated HT-22 neurons (Fig. 3). Various concentrations (50, 100, 200 and 400 µg/ml) of CPE were incubated for 2 h with DPPH in cell-free system. The amounts of DPPH radicals were spectrophotometrically determined, which indicate radical scavenging activities. The results of DPPH assays showed that CPE (50, 100, 200 and 400 µg/ml) have marked ROS-scavenging activity in cell-free system in a dose-dependent manner (Fig. 3-A). The fluorescence spectrometric data from DCF-DA assays revealed that CPE treatment (200 µg/ml, 1 h) significantly attenuated the intracellular ROS levels by 44.6±1.6% (Fig 3-B) in H₂O₂ (1 mM, 30 min)-stimulated neurons. Additionally, we evaluated the enzyme activities of catalases and SOD, which are important antioxidant intracellular enzymes. CPE treatment (200 µg/ml, 1 hr) protected HT-22 neurons from H₂O₂ (1 mM, 30 min)-induced deterioration of these enzyme activities by 81.9±4.5% and 98.5±27.7%, respectively (Fig 3-C and D).

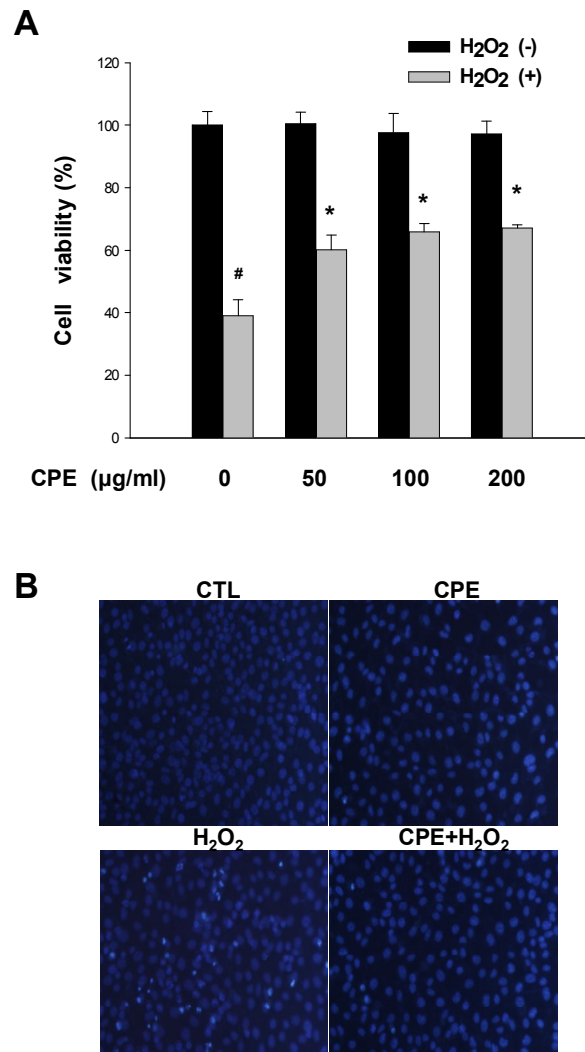


Fig. 1. Neuroprotective effects of CPE against H₂O₂-induced oxidative neurotoxicity.

A. HT-22 neurons were treated with H₂O₂ (1 mM) for 12 h in the presence or absence of CPE (50, 100 and 200 µg/ml). CPE was pretreated for 1 hr before H₂O₂ stimulation. The neuroprotective effects of the CPE were evaluated using MTT cell viability assays. B. Chromatin condensation as an apoptotic nuclear appearance was observed under a fluorescent microscope after Hoechst 33342 staining. #, $p < 0.05$ as compared to the untreated controls and *, $p < 0.05$ as compared to the group treated with H₂O₂ alone. Scale bar, 100 µm.

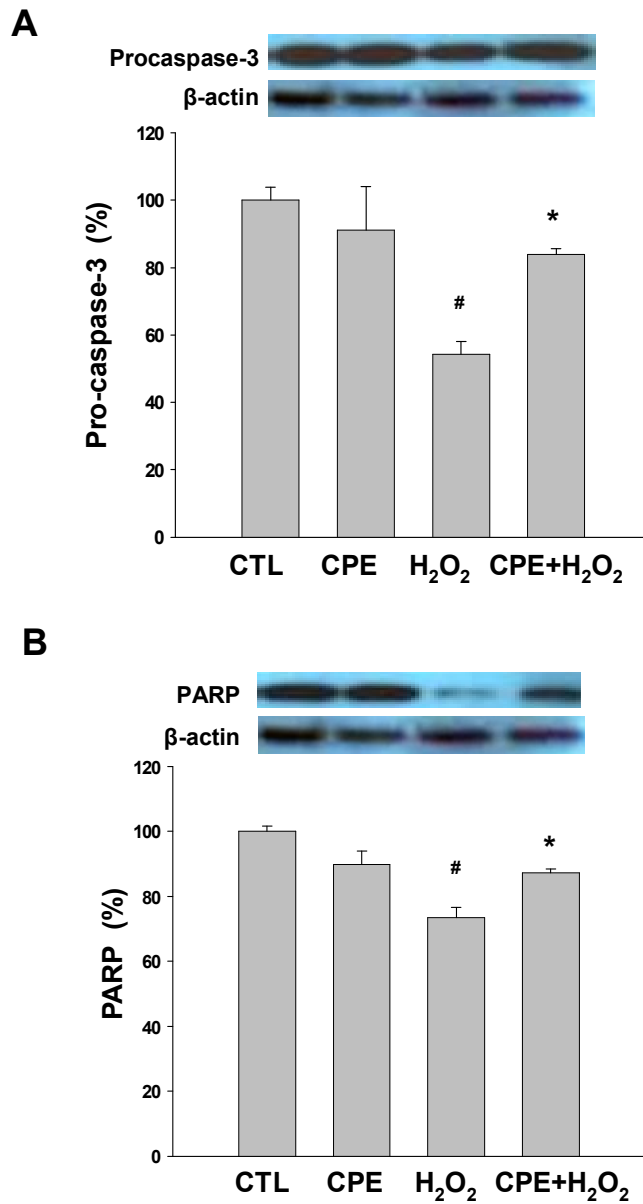


Fig.2. Effect of CPE on procaspase-3 and PARP against H₂O₂-induced oxidative neurotoxicity

The effects of CPE on procaspase-3 (A) and PARP (B) expression levels were determined via Western blotting analyses. Groups were compared with % of untreated control group. #, $p < 0.05$ as compared to the untreated controls and *, $p < 0.05$ as compared to the group treated with H₂O₂ alone.

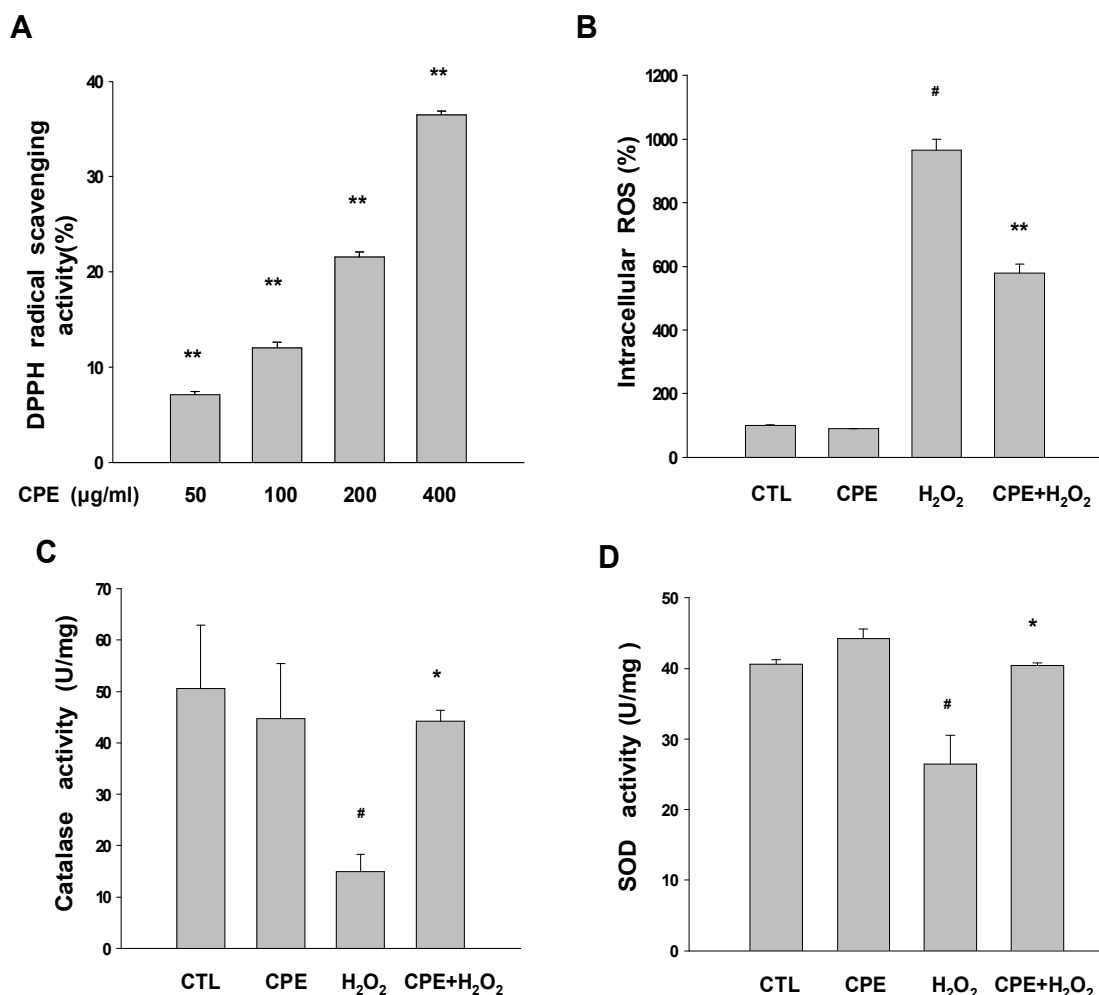


Fig.3. Anti-oxidant activities of CPE.

A. Various concentrations (50, 100, 200 and 400 µg/ml) of CPE were incubated for 2 h with DPPH in cell-free system. The amounts of DPPH radicals were spectrophotometrically determined, which indicate radical scavenging activities. B. HT-22 neurons were treated with H₂O₂ (1 mM) for 30 min in the presence or absence of CPE (200 µg/ml). CPE was pretreated for 1 hr before H₂O₂ stimulation. Then intracellular ROS levels were detected using a spectrofluorometer using DCF-DA. C-D. The effects of CPE on enzyme activities of catalase (C) and SOD (D) were measured with a spectrophotometer. #, $p < 0.05$ as compared to the untreated control group and *, $p < 0.05$; **, $p < 0.01$ as compared to the group treated with H₂O₂ alone.

3.3. Mild-depolarizing effects of CPE on $\Delta\Psi_m$

We evaluated the effects of CPE on $\Delta\Psi_m$ in resting neurons using real-time fluorescence recording analyses. TMRM is a cell-permeant, cationic fluorescent probe that is sequestered by mitochondria in proportion to $\Delta\Psi_m$ (Scaduto and Grotyohann, 1999). The cells on poly-L-lysine-coated cover glasses were loaded with 100 nM TMRM for 30 min, washed for three times and mounted on a recording chamber of an epifluorescence inverted microscope Olympus IX71 (Olympus, Japan). TMRM fluorescence values from individual cells were normalized to the value before drug treatment and traces shown in Fig. 4-A show average recordings of TMRM fluorescence intensities.

Treatment of TMRM-loaded cells with CPE induced a dose (100, 200 and 400 $\mu\text{g/ml}$)-dependent decrease in TMRM fluorescence intensities, indicating mild mitochondrial depolarization (Fig. 4). The mitochondrial uncoupler CCCP (10 μM) markedly decreased TMRM fluorescence intensity, which means total $\Delta\Psi_m$ dissipation. At 10 min-time point after drug treatment, the normalized TMRM fluorescent intensities were 71.7%, 67.6%, 62.2%, 41.3%, 10.9% in control, CPE (100, 200 and 400 $\mu\text{g/ml}$) and CCCP (10 μM)-treated groups, respectively (Fig. 4-B). These data indicate that mitochondria-depolarizing activity of CPE was significantly smaller than that of the uncoupler CCCP. This CPE-induced partial depolarization of mitochondrial membrane should be fundamentally distinguished from $\Delta\Psi_m$ dissipation, which means a full-blown mitochondrial depolarization at the almost final stage in mitochondria-dependent apoptotic pathways. This mild mitochondrial depolarization has been recently evaluated as a novel mechanism of neuroprotection via inhibiting mitochondrial Ca^{2+} overload during neuronal insults (Garcia-Martinez *et al.*, 2010; Sanz-Blasco *et al.*, 2008; Storozhevych *et al.*, 2010).

JC-1 is another cationic fluorescent probe which exhibits $\Delta\Psi_m$ -dependent accumulation in the mitochondria and has different optical properties from TMRM (See 'Materials and

methods'). Therefore, we tried to investigate CPE effects on $\Delta\Psi_m$ with JC-1 in addition to TMRM. As mitochondrial membrane depolarization is also indicated by a reduction in the JC-1 aggregate forms (red) to JC-1 monomers (green) ratio of JC-1 fluorescence intensities, we evaluated the effects of CPE on the JC-1 ratio using flow cytometric analyses (Fig. 5-B) and confocal microscopy (Fig. 5-A), in addition to real-time fluorescence measurement with TMRM (Fig. 4). HT-22 neurons were treated with CPE (200 $\mu\text{g}/\text{ml}$, 1 h), subsequently loaded for 30 min with JC-1 fluorescent indicator (2 μM) and analyzed with a flow cytometer. This flow cytometric data with JC-1 (Fig. 5) indicate that CPE treatment resulted in a partial depolarization of the mitochondrial membrane, consistent with $\Delta\Psi_m$ data using TMRM (Fig. 4). The confocal microscopic images for $\Delta\Psi_m$ visually demonstrated the reduction of red to green ratio of JC-1 fluorescence intensities after treatments of CPE (Fig. 5-A), consistent with quantitative flow cytometric data with JC-1 (Fig. 5-B).

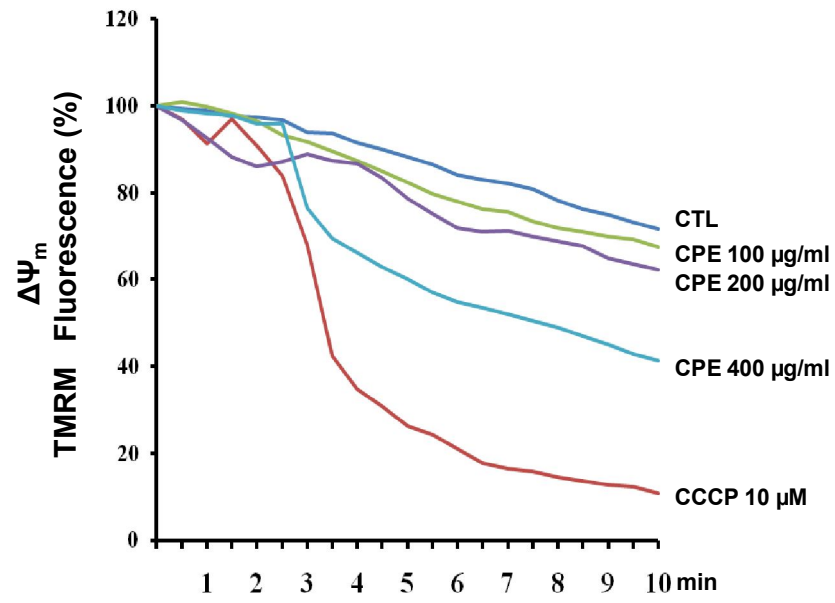
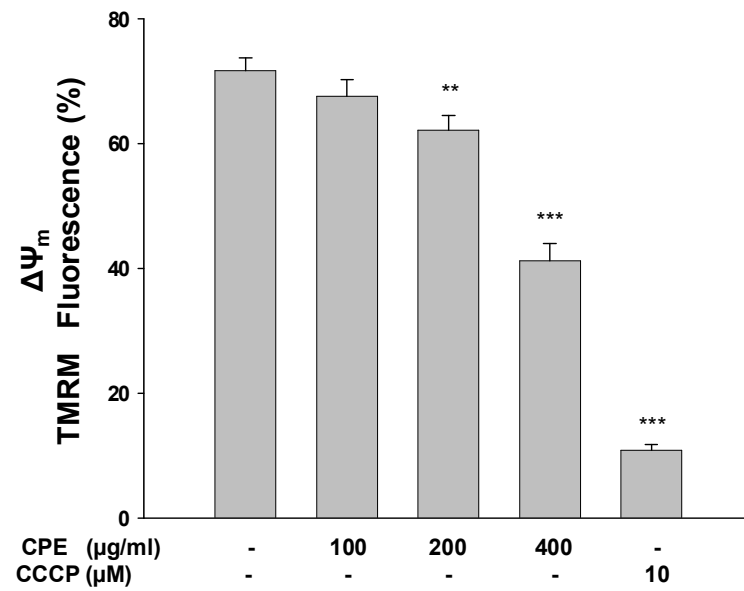
A**B**

Fig.4. CPE evokes a mild mitochondrial depolarization, as indicated in real-time measurement of $\Delta\Psi_m$.

A. Real-time measurement of $\Delta\Psi_m$ was conducted with MetaFluor software using a cationic fluorescent probe TMRM that is sequestered by mitochondria in proportion to $\Delta\Psi_m$. A decrease in TMRM fluorescence reflects mitochondrial depolarization. The cells on poly-L-lysine-coated cover glasses were loaded with 100 nM TMRM for 30 min, washed for three times and mounted on a recording chamber of an epifluorescence inverted microscope Olympus IX71. Various doses (100, 200 and 400 $\mu\text{g/ml}$) of CPE were superfused on TMRM-loaded HT-22 neurons in recording chamber to evaluate CPE effects on $\Delta\Psi_m$. TMRM fluorescence values from individual cells were normalized to the value before drug treatment and averaged (n=12 cells). Traces show average recordings of TMRM fluorescence intensities. B. Quantification of TMRM fluorescence. At 10 min-time point after drug treatment, the normalized TMRM fluorescent intensities were compared among controls, CPE (100, 200 and 400 $\mu\text{g/ml}$) and CCCP (10 μM)-treated groups. **, $p<0.01$; ***, $p<0.001$ as compared to controls.

3.4. Differential effects of single compounds of CPE on $\Delta\Psi_m$

The major flavonoids of CPE (Table. 1) were investigated to explore single compounds responsible for CPE effects on $\Delta\Psi_m$. Since HPLC analyses showed that CPE contained abundant flavonoids, such as rutin (5.32 mg/g), hesperidin (14.15 mg/g), nobiletin(8.67 mg/g), tangeretin (14.52 mg/g), sinensetin (0.91 mg/g).

The normalized ratios of red (JC-1 aggregate) to green (JC-1 monomers) fluorescence intensities (F_{red}/F_{green} ratio) of JC-1 were $56.6\pm 4.5\%$, $73.8\pm 0.6\%$, $67.9\pm 0.6\%$, $78.8\pm 1.7\%$, $98.2\pm 1.9\%$ and $95.7\pm 6.1\%$, respectively in CCCP (10 μM , 30 min), CPE (200 $\mu\text{g}/\text{ml}$, 1 hr), nobiletin (50 μM , 1 h), tangeretin (50 μM , 1 h), rutin (50 μM , 1 h), and hesperidin (50 μM , 1 h)-treated groups compared to control group (Fig. 2-A). This flow cytometric data indicate that only polymethoxylated flavones such as nobiletin and tangeretin were capable of inducing a mild mitochondrial depolarization, while rutin as flavonol glycosides and hesperidin as flavanone glycosides did not affect on $\Delta\Psi_m$. These results suggest that single compounds responsible for CPE effects on $\Delta\Psi_m$ are polymethoxylated flavones such as nobiletin and tangeretin.

Table 1. Flavonoids content (mg/g) contained in CPE.

| Flavonoid | Rutin | Naringin | Hesperedin | Quercetin | Naringenin | Hesperetin | Sinensetin | Nobiletin | Tangeretin |
|-----------|-------|----------|------------|-----------|------------|------------|------------|-----------|------------|
| Mean | 5.32 | ND | 14.15 | ND | ND | ND | 0.91 | 8.67 | 14.52 |
| RSD | 0.15 | - | 0.24 | - | - | - | 0.03 | 0.28 | 0.57 |

RSD, relative standard deviation (%)

ND, not detected

The numbers are the means calculated from three experiments

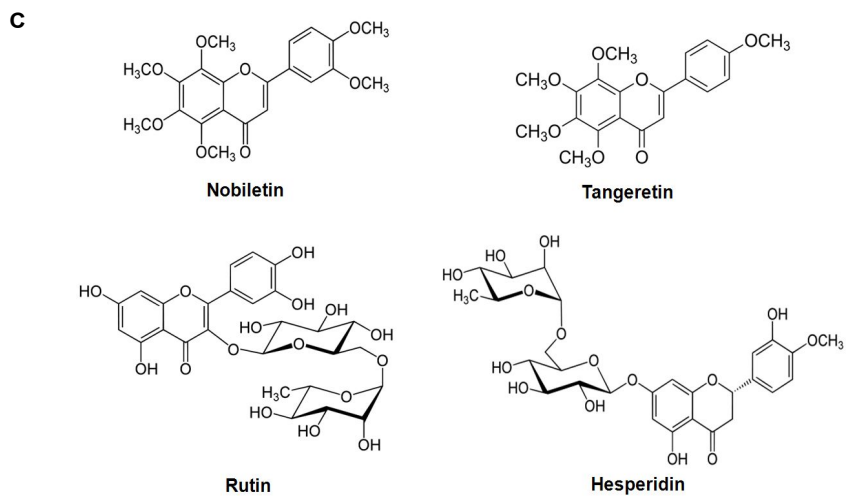
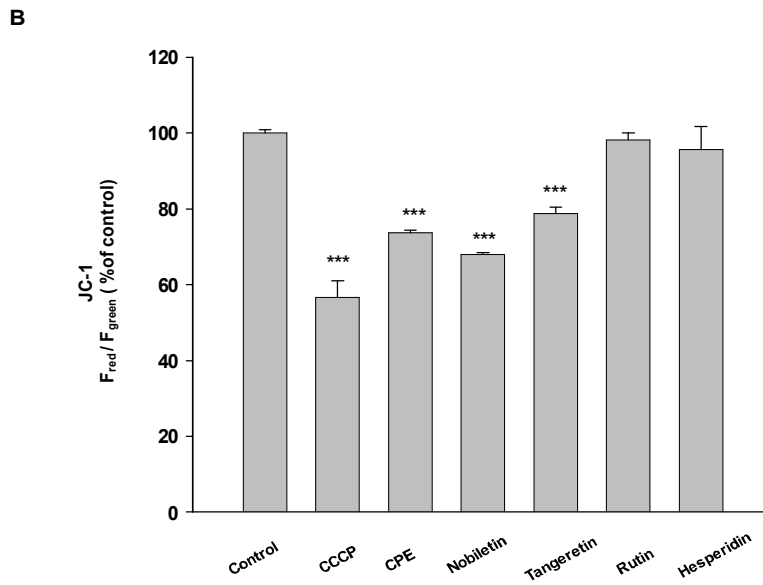
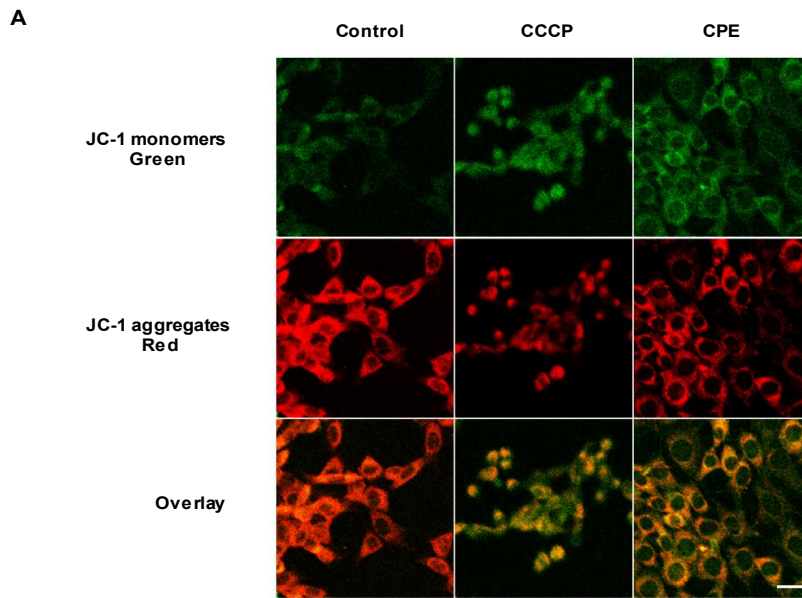


Fig 5. Differential effects of single compounds of CPE on JC-1 F_{red}/F_{green} ratio indicative of $\Delta\Psi_m$.

A. The major flavonoids of CPE were investigated to explore single compounds responsible for CPE effects on $\Delta\Psi_m$. HT-22 neurons were treated with CCCP (10 μM , 30 min), CPE (200 $\mu\text{g}/\text{ml}$, 1 hr), nobiletin (50 μM , 1 h), tangeretin (50 μM , 1 h), rutin (50 μM , 1 h), and hesperidin (50 μM , 1 h), subsequently loaded for 30 min with JC-1 (2 μM). The red (JC-1 aggregates) to green (JC-1 monomers) fluorescence ratio of JC-1 were measured using flow cytometry analyses to evaluate the effects on $\Delta\Psi_m$ and normalized compared to values in untreated control group. A decrease in JC-1 F_{red}/F_{green} ratio indicates mitochondrial depolarization. ***, $p < 0.001$ as compared to controls. B. The representative confocal microscopic images for $\Delta\Psi_m$ were shown by the JC-1 dual emission of red and green fluorescences. The upper panels for JC-1 green fluorescent emission, the middle panels for JC-1 red fluorescent emission, and the lower panels for the overlay of green and red ones. Scale bar, 100 μm . C. Chemical structures of major flavonoids contained in CPE.

3.5. Inhibitory effects of CPE on H₂O₂-induced overload of Ca²⁺ in both the cytosol and the mitochondria

Ca²⁺ deregulation of intracellular Ca²⁺ homeostasis is known to be involved in pathological processes such as oxidative neurotoxicity (Feissner *et al.*, 2009). Therefore, we investigated the regulatory effect of CPE (10, 100, 200 and 400 µg/ml) on Ca²⁺ deregulation in H₂O₂ (1 mM, 30 min)-induced oxidative neurotoxicity. Flow cytometric analyses were accomplished using Fluo-4 AM and Rhod-2 AM fluorescent indicators for cytosolic and mitochondrial Ca²⁺, respectively. H₂O₂ treatment remarkably increased both cytosolic and mitochondrial Ca²⁺ levels ([Ca²⁺]_i and [Ca²⁺]_m) and the H₂O₂-induced increases in Ca²⁺ levels were significantly attenuated by CPE treatment (200 µg/ml) in both the cytosol and the mitochondria, by 26.6±0.7% and 27.0±1.7%, respectively (Fig. 5-A). These inhibitory effects of CPE (10, 100, 200 and 400 µg/ml) on both cytosolic and mitochondrial Ca²⁺ levels were dose-dependent, showing a bell-shaped dose-response relation. The maximal inhibitions were shown in 200 µg/ml of CPE treatment (Fig. 5-B). Fig. 5-C provides representative confocal microscopic images demonstrating the inhibitory effect of CPE on H₂O₂-induced mitochondrial overload of Ca²⁺, indicated by rhod-2 fluorescence.

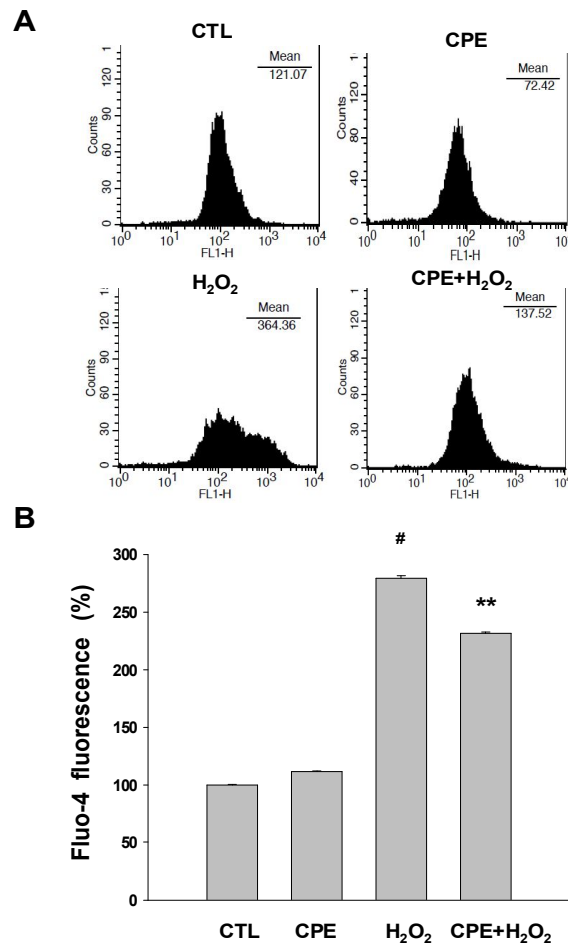


Fig.6. Inhibitory effects of CPE on cytosolic Ca²⁺ overload.

A and B After pretreatment of CPE for 1 h, HT-22 neurons were treated with H₂O₂ (1 mM, 30 min) in the presence or absence of CPE (200 µg/ml), then loaded for 30 min with Fluo-4 AM (5 µM) for the measurement of cytosolic Ca²⁺ level. The fluorescent intensities were immediately evaluated via flow cytometric analyses. The inhibitory effects of CPE on H₂O₂-induced overload of Ca²⁺ in cytosol. Groups were compared with % of untreated control group. #, *p*<0.05 as compared to the untreated controls and *, *p*<0.05; **, *p*<0.01, as compared to the group treated with H₂O₂ alone.

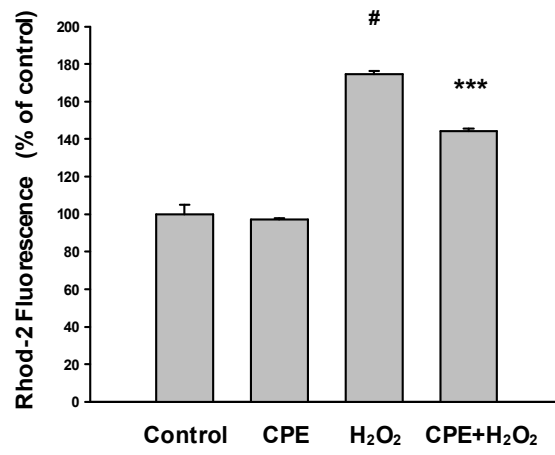
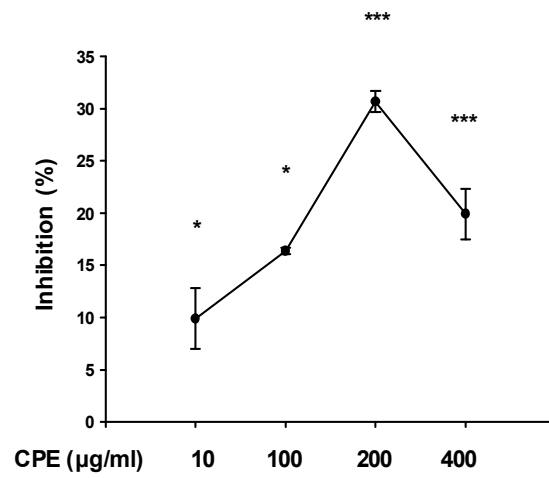
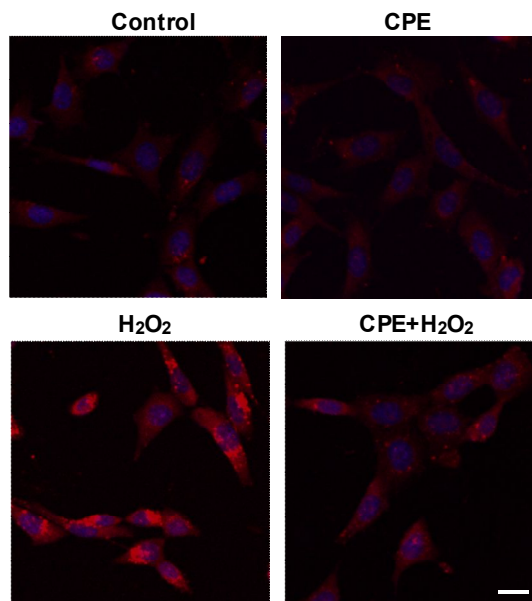
A**B****C**

Fig.7. Inhibitory effects of CPE on H₂O₂-induced mitochondrial calcium overload.

A. After pretreatment of CPE for 1 h, HT-22 neurons were treated with H₂O₂ (1mM, 30 min) in the presence or absence of CPE (200 µg/ml), then loaded for 30 min with Rhod-2 AM (5 µM) for the measurement of mitochondrial Ca²⁺ levels. The fluorescent intensities were immediately evaluated via flow cytometric analyses. B. Dose (10, 100, 200 and 400 µg/ml)-response relations of the inhibitory effects of CPE on H₂O₂-induced overload of Ca²⁺ in mitochondria. C. The representative confocal microscopic images demonstrating the inhibitory effect of CPE on H₂O₂-induced mitochondrial overload of Ca²⁺, indicated by rhod-2 fluorescence. Nuclear counterstaining was accomplished with DAPI. Groups were compared by % of untreated control group. #, *p*<0.05 as compared to the untreated controls and *, *p*<0.05; ***, *p*<0.001, as compared to the group treated with H₂O₂ alone. Scale bar, 100 µm.

4. Discussion

In this study, we investigated the neuroprotective mechanism of CPE against oxidative neurotoxicity. Treatment with CPE markedly increased neuronal viability in an H₂O₂-induced oxidative neurotoxicity model using HT-22 cells (Fig. 3-A and B). Additionally, CPE treatment inhibited neuronal apoptosis cascades including caspase 3 and PARP (Fig. 3-C and D). CPE treatment demonstrated the robust anti-oxidant activity of ROS scavenging (Fig. 4), and significantly blocked H₂O₂-induced mitochondria Ca²⁺ overload in both the cytosol and the mitochondria (Fig. 5) and induced a mild depolarization of the mitochondrial membrane (Fig. 1 and 2). Taken together, the results of the present study suggest dual mechanisms underlying the neuroprotective effects of CPE: these dual mechanisms involves both anti-oxidant activity and partial blockade of mitochondrial Ca²⁺ overload due to the mild depolarization of the mitochondrial membrane.

The flow cytometric data indicate that only polymethoxylated flavones (PMFs) such as nobiletin and tangeretin were capable of inducing a mild mitochondrial depolarization, while rutin as flavonol glycosides and hesperidin as flavanone glycosides did not affect $\Delta\Psi_m$. These results suggest that single compounds responsible for CPE effects on $\Delta\Psi_m$ are PMFs such as nobiletin and tangeretin. PMFs, are flavones bearing two or more methoxy groups on their basic benzo-c-pyrone (15-carbon, C6–C3–C6) skeleton with a carbonyl group at the C4 position (Li *et al.*, 2009). PMFs were shown to the most potentially inhibit NO release in lipopolysaccharide(LPS)-stimulated RAW 264.7 murine macrophage cell line out of *Citrus* peel flavonoids, suggesting stronger anti-inflammatory activity than any other *Citrus* peel flavonoids (Choi *et al.*, 2007). PMFs are the most commonly investigated due to their outstanding biological activities out of *Citrus* flavonoids. The possible targets by which PMFs regulate $\Delta\Psi_m$ might be mitochondrial channels/transporters, or possibly the components of electron transport chains. The underlying mechanism how PMFs induces

mild mitochondrial depolarization remains unclear, and should be elucidated in future studies.

The balance of ROS levels between generation and scavenging is crucial to cellular functions and homeostasis. However, excessively high levels of ROS activate the apoptotic cascades through mitochondrial dysfunction. ROS-induced mitochondria dysfunction involves ATP depletion, $\Delta\Psi_m$ dissipation, MPTP opening, and cytosolic cytochrome C release. These cascades activate caspase 9 and caspase 3 in turn, and then the activated caspase 3 degrades important proteins, including the DNA repair-related enzyme PARP. These apoptotic processes are referred to as the intrinsic pathway or the mitochondria-dependent pathway.

Hydrogen peroxide (H_2O_2) is a freely diffusible form of ROS through the cell membrane and is produced by many intracellular reactions, and is implicated in apoptosis in various cells. H_2O_2 treatment is the most commonly used experimental model of oxidative cytotoxicity. H_2O_2 treatment induces excess generation of ROS such as the superoxide ($O_2^{\cdot-}$) and hydroxyl radical ($\cdot OH$), which subsequently result in mitochondrial dysfunction and ATP depletion (Ishimura *et al.*, 2008). Intracellular ATP depletion induces the dysfunction of ATP-dependent ionic pumps. Dysfunction of Na^+K^+ ATPases evokes cell membrane depolarization and increases $[Ca^{2+}]_i$ due to activation of voltage-gated Ca^{2+} channels and a reversed operation of the Na^+Ca^{2+} exchanger (Wang *et al.*, 2003). In addition, sarcoplasmic reticulum Ca^{2+} ATPases (SERCA), and plasma membrane Ca^{2+} ATPases (PMCA) are susceptible to ATP depletion, all of which are involved in the increase of $[Ca^{2+}]_i$ (Clapham, 1995). It is known that the cytosolic Ca^{2+} overload ultimately results in the uptake of Ca^{2+} into the mitochondria (Rizzuto *et al.*, 2009). Therefore, H_2O_2 treatment increases both $[Ca^{2+}]_i$ and $[Ca^{2+}]_m$, as shown in Fig. 5.

The physiological level of mitochondrial Ca^{2+} regulates intracellular Ca^{2+} signals as well as the rate of ATP synthesis through the tricarboxylic acid (TCA) cycle-associated metabolic enzymes (i.e., pyruvate, alpha-ketoglutarate and isocitrate dehydrogenases) (Jouaville *et al.*, 1999; Lasorsa *et al.*, 2003). However, excess mitochondrial Ca^{2+} overload is crucial to

trigger neuronal apoptosis by opening the mPTP, evoking cytochrome C release, activating caspase cascades, and ultimately inducing cell death (Pinton *et al.*, 2008).

In this study, we demonstrated that CPE treatment significantly reduced H₂O₂-induced increases in the levels of cytosolic and mitochondrial Ca²⁺ (Fig. 5). The inhibitory effects of CPE on cytosolic Ca²⁺ levels are attributed principally to their ROS scavenging activity, because excess intracellular ROS-induced mitochondrial dysfunction increases cytosolic Ca²⁺ levels. It is known that the cytosolic Ca²⁺ overload ultimately results in the uptake of Ca²⁺ into the mitochondria. However, the inhibitory effect of CPE on mitochondrial Ca²⁺ overload is difficult to explain with single mechanism because inhibiting of H₂O₂-induced cytosol Ca²⁺ overload finally reduces mitochondrial Ca²⁺ overload.

Taken together, we suggest that CPE may exert neuroprotective activities against oxidative neurotoxicity implicated in neurodegenerative diseases. The neuroprotective mechanism is associated with the intrinsic ability of CPE to induce mild mitochondrial depolarization as well as with its anti-oxidant activities. These findings might raise the recent issue of a novel role of mild mitochondrial depolarization in neuroprotection.

PART II

**A novel neuroprotective mechanism of
indomethacin against excitotoxicity
via mitochondrial K_{ATP} in the primary
cortical neurons**

1. Introduction

Indomethacin is a NSAID commonly used to reduce fever, pain and swelling. It was a potent, nonselective inhibitor of the cyclooxygenase enzymes (COX-1 and COX-2) and is a powerful anti-inflammatory agent and also exhibits anticancer activity as suggested by a report demonstrating that indomethacin significantly increased the lifespan of terminally ill patients suffering from a range of cancers (Lundholm *et al.*, 1994). The neuroprotective effects of the minocycline, NSAIDs, and KB-R7943 (Storozhevyykh *et al.*, 2010) against excitotoxic insults have recently been proposed to be attributable to their intrinsic ability to induce mitochondrial depolarization in resting neurons. $\Delta\Psi_m$ is evaluated as a potent target to modulate mitochondrial Ca^{2+} overload which might be the triggering point of neuronal cell death.

Steady-state Ca^{2+} level within mitochondria of living cells have many physiological functions. 1) Activation of dehydrogenases in TCA cycle, respiratory chain and ATP synthesis. 2) Buffering local cytosolic Ca^{2+} rises. 3) Inducing mPTP opening and cell death (Pizzo *et al.*, 2012). But in many neuronal insults, mitochondria calcium overload induces the collapse of $\Delta\Psi_m$, opening of the mPTP and release of pro-apoptotic factors to trigger cell death. The exact molecular composition of mPTP is unknown, but possible regulation components, such as adenine nucleotide transporter (ANT), voltage-dependent anion channel (VDAC), and cyclophilin D were shown to be directly or indirectly involved in mPTP opening (Crompton, 1999).

Owing to a growing body of evidences, mitochondrial potassium channels, especially mitK_{ATP} , are believed to be involved in cytoprotection of injured cardiac and neuronal tissues (Liu *et al.*, 1999) (Garlid *et al.*, 2003). K_{ATP} is a potassium channel which is inactivated by ATP. The molecular identity of the K_{ATP} channel is still unclear. It is believed that K_{ATP} channels are composed of a pore-forming subunit (Kir6.2 subunit) and a mitochondrial sulfonylurea receptor (mitoSUR) (Choma *et al.*, 2009). It is located in various parts of the

cell, including the plasma membrane (sK_{ATP}) and inner mitochondrial membrane ($mitoK_{ATP}$). Function of K_{ATP} channel opening will depend upon location: activation of sK_{ATP} leads to hyperpolarization of cells while opening of $mitoK_{ATP}$ causes depolarization of mitochondria. The $mitoK_{ATP}$ channel was first identified using the patch clamp technique in rat liver mitochondria (Inoue *et al.*, 1991). Previously, the properties of brain mitochondrial $mitoK_{ATP}$ channels were also determined using isolated mitochondria (Bajgar *et al.*, 2001). It was demonstrated that a physiological role of the $mitoK_{ATP}$ channels is to buffer potential perturbations of matrix volume and the intermembrane space so that ATP production and transport are at optimal levels for cellular needs (Busija *et al.*, 2004).

In the present study, we investigated the neuroprotective effect of indomethacin, a non-steroidal anti-inflammatory drug on glutamate-induced excitotoxicity model. And we also examined if 5HD, a specific $mitK_{ATP}$ channel blocker, abolishes the protection by indomethacin in cultured cortical neuron.

2. Materials and methods

2.1. Materials

Minimum Essential Medium (MEM), Neurobasal Medium, fetal bovine serum (FBS), penicillin/streptomycin, B-27 Serum-Free Supplement were purchased from Gibco BRL(Grand Island, NY, USA). Tetramethylrhodamine ethyl ester (TMRE), Fura-2 acetoxymethyl ester (Fura-2 AM), rhod-2 acetoxymethyl ester (Rhod-2 AM), Imag-It live Mitochondrial Transition Pore Assay Kit and MitoSOX Red were purchased from Invitrogen (Carlsbad, CA, USA). We purchased anti-cytochrome C from Santa Cruz Biotechnology (Santa Cruz, CA, USA) and Alexa 488 a rabbit IgG were purchased from Invitrogen (Invitrogen Barcelona, Spain). All other reagents were purchased from Sigma-Aldrich (St Louis, MO, USA), unless indicated otherwise.

2.2. Cell culture

All animal experiments were approved by the Institutional Review Board (IRB) of animal, Jeju University College of Medicine, and the procedure was carried out in accordance with the guidelines of the IRB. Primary cortical neuronal culture was obtained from 20-day-old embryonic Sprague-Dawley rats. The cortex was dissected and placed in ice-cold Ca^{2+} free Normal Tyrode solution. Then the cortex was removed to Plating Media (MEM supplemented with 10% FBS, 0.45% Glucose, 1 mM sodium pyruvate and penicillin/streptomycin) and dissociated by glass pasteur pipettes. Then cortical neuron cells were plated onto poly-L-lysine coated glass coverslips and maintain at 37°C in a humidified atmosphere of 5% CO_2 . After six hours later, aspirate plating medium and add neurobasal medium to each well and change the media twice for week. In some experiment, at 4th day,

cultures were treated with 1 μ M arabinofuranosyl cytidine (Ara-C) to prevent glial proliferation. Neurons at 10-13 DIV were used for the experiments.

2.3. Immunofluorescence microscopy and labeling of mitochondria

Cells were treated under the various experimental conditions and then fixed in 4% paraformaldehyde for 30 min and permeabilized in PBS containing 0.5% Triton X-100 in PBS for 10 min twice at room temperature. Following blocking incubation in 5% normal goat serum in PBS for 1 h. Neurons were incubated at room temperature for 2 h with anti-Tuj-1 or anti-NeuN (1:200) in 5% NGS in PBS. Then the coverglass were exposed to green-fluorescent Alexa Fluor 488 anti-rabbit IgG (1:200) for 1 h at room temperature. After washing and mount with Prolong antifade kit solution with DAPI. In some experiment, 0.2 μ M Mito Tracker Red was been used to labeling of mitochondria. The fluorescence images were captured by an epifluorescence inverted microscope Olympus IX71 (Olympus, Japan) and MetaMorph (Molecular Devices, CA, USA) software.

2.4. Measurement of cell viability

MTT [3-(4,5-dimethylthiazol-2-yl)-2,5-diphenyl tetrazolium bromide] was used to examine the effect on cell viability, as previously described (Cui *et al.*, 2010). After treatment, MTT was added to the cultured medium and incubated for 2 h at 37°C. Then, medium was removed, and DMSO was added to dissolve formazan. After gently shaking, absorbance was subsequently read at 540 nm using a microplate reader (Model 550, Bio-Rad, USA).

2.5. Real-time measurement of $\Delta\Psi_m$

The cells on poly-L-lysine-coated cover glasses were loaded with 25 nM TMRM for 10 min, washed for three times and mounted on a recording chamber of an epifluorescence inverted microscope Olympus IX71 (Olympus, Japan). Digitized fluorescence images were acquired at 30 s intervals with a cooled-charge device (CCD) camera (Cascade, Roper Scientific, USA), and analyzed in a personal computer using Metafluor software (Molecular Devices, CA, USA). During recording, the cells were superfused with Normal Tyrode solution by fast flow system using tubing. Normal Tyrode solution contained (mM): 145 NaCl, 1.3 MgCl₂, 2 CaCl₂, 5 KCl, 10 HEPES, 10 glucose. Drug application was accomplished by changing perfusion medium.

2.6. Dual recording for Cytosolic and mitochondrial Ca²⁺

For simultaneous fluorescence imaging of cytosolic Ca²⁺, neurons were loaded for 45 min in the cell culture medium at 37°C with Fura-2 AM (5 μM) and Pluronic F127 (0.1%). For mitochondrial calcium measurement, Rhod-2 AM (2 μM) was used and incubated the cells at 4°C for 45 min. After washing, the cell was transferred to the recording chamber for acquisition. Fluorescence was excited with the high speed filter changer of 340 nm, 380 nm, 548/20 nm wavelengths using a rapidly tunable (<1.2msec wavelength change) with Lamber DG4 (Sutter Instrument, Novato, CA) and D510/80m emitter filter (Chroma Technology). Digitized fluorescence images were acquired at 6 s intervals with a cooled-charge device (CCD) camera (Cascade, Roper Scientific, USA), and analyzed in a personal computer using Metafluor software (Molecular Devices, CA, USA). The changes in cytosolic and mitochondrial calcium were normalized to the baseline fluorescence at the beginning.

2.7. DPPH radical scavenging assay

Various concentrations of CPE (10 μ l) were added to 190 μ l (0.15 mM in ethanol) of DPPH (1,1-diphenyl-2-picrylhydrazyl radical) and vigorously mixed. The mixture was incubated for 1 h in darkness at room temperature, and the absorbance was read at 517 nm using a microplate reader (Sunrise, Tecan, Austria). The percentage level of DPPH scavenging was calculated according to the following formula: % Radical Scavenging = $[(A - A_s)/A] \times 100$, in which A is the absorbance of DPPH and A_s is its absorbance after citrus peel extract treatment.

2.8. Intracellular reactive oxygen species (ROS) measurement

The cells were seeded on 96-well tissue culture plates at 2×10^4 cells/well and pretreated for 30 min with CPE followed by 1 mM H_2O_2 for an additional 30 min. After the addition of 50 μ M of DCF-DA (2',7'-dichlorodihydrofluorescein diacetate), fluorometric analysis was conducted at an excitation/emission wavelength of 485 nm/535 nm using a microplate reader (Spectra Fluor, Tecan, Austria).

2.9. Real-time measurement of mitochondrial superoxide generation

The cells on poly-L-lysine-coated cover glasses were loaded with 5 μ M MitoSOX Red for 10 min, washed and mounted on a recording chamber of an epifluorescence inverted microscope Olympus IX71 (Olympus, Japan). Digitized fluorescence images were acquired at 30 s intervals with a cooled-charged device (CCD) camera (Cascade, Roper Scientific, USA), and analyzed in a personal computer using Metafluor software (Molecular Devices, CA, USA).

2.10. Mitochondrial permeability transition pore (mPTP) assay

mPTP opening was assessed directly by the calcein/cobalt method according to the manufacturer's protocol. Calcein AM a nonfluorescent esterase substrate, can passively diffuse into the cells and accumulates in cytosolic compartment, including mitochondria. After loading, intracellular esterase cleaves the acetoxymethyl esters to liberate fluorescent dye calcein, which does not cross the mitochondrial or plasma membranes. To quench fluorescence of cytosolic calcein, CoCl_2 was added to the media to maintain only mitochondrial calcein fluorescence. Cells were co-loaded with calcein-AM 1 μM and CoCl_2 1 mM for 30 min at 37°C. The cells then subjected to inverted microscope Olympus IX71 (Olympus, Japan) and MetaMorph (Molecular Devices, CA, USA) software.

2.11. Statistics analysis

Data are expressed as mean value \pm standard error of the mean (SEM). Statistical analyses were conducted using Student's *t*-test. The differences between groups were regarded as statistically significant when $p < 0.05$.

3. Results

3.1. Purity of primary cortical neuron

Cells, at 10-15 DIV were used in our study. In real time recording, neurons were easily distinguishable from glia in morphology. Under microscopy, neurons had smooth rounded soma and distinct processes and lay just above the focal plane of the glial layer. To get a pure neuron in some experiments except real time recording, cultures were treated with 1 μ M arabinofuranosyl cytidine (Ara-C) to prevent glial proliferation. Therefore we investigated the purity of neurons in our culture system using immunofluorescence microscopy using anti-Tu-j1 (Fig. 8-A) and anti-NeuN (Fig. 8-B) which was specific neuronal microtubules marker and neuronal nuclear marker. Neurons were counted in the presence or absence of Ara-C and their purities of neuron were 95.2 ± 2.5 % and 25.1 ± 5.0 % respectively (Fig. 8-C).

3.2. Mitochondrial K_{ATP} channel blockade abolishes neuroprotective effect of indomethacin on glutamate-induced neurotoxicity in primary cortical neuron

To induce a calcium dependent excitotoxic cell death, we exposed cultured cortical neurons to glutamate (100 μ M) and glycine (10 μ M) for 30 min. Treatments were terminated by washing cells three times before incubating with regular medium. Cell viability was analyzed 24 h later via MTT assays. Neurons were treated with glutamate(100 μ M) for 30 min in the presence or absence of indomethacin. Pretreatment with various concentrations (10, 30) of indomethacin were carried out for 5 min prior to glutamate expose. Indomethacin treatments markedly increased cell viability against glutamate-induced neurotoxicity to $41.6\pm 4.0\%$, and $50.0\pm 5.6\%$ respectively in a dose- dependent manner, relative to the group

treated with glutamate alone was $32.8 \pm 1.7\%$ (Fig. 9-B). Indomethacin alone evidenced no cytotoxicity at concentrations below $50 \mu\text{M}$ (Fig. 9-A). Treatment of 5HD ($500 \mu\text{M}$), a specific $\text{mitoK}_{\text{ATP}}$ channels blocker partially abolished these protective effects of indomethacin. These data indicate that $\text{mitoK}_{\text{ATP}}$ may be regulate neuroprotective effect of indomethacin.

3.3. Mitochondrial K_{ATP} channel blockade abolishes neuroprotective effect of indomethacin on glutamate-induced ROS generation

In the next study, we investigated the antioxidant activities of indomethacin. Various concentrations (1, 10, 50 and $100 \mu\text{M}$) of indomethacin were incubated for 2 h with DPPH in cell-free system. The amounts of DPPH radicals were spectrophotometrically determined, indicating radical scavenging activities. The results of DPPH assays showed that indomethacin did not have a ROS-scavenging activity in cell-free system (Fig. 10-A). While the fluorescence spectrometric data from DCF-DA assays revealed that indomethacin treatment ($30 \mu\text{M}$) significantly attenuated the intracellular ROS levels (Fig 10-B) in glutamate ($100 \mu\text{M}$)-stimulated neurons. Therefore, these results indicate that neuroprotective effect of indomethacin is not caused by antioxidant activity of indomethacin.

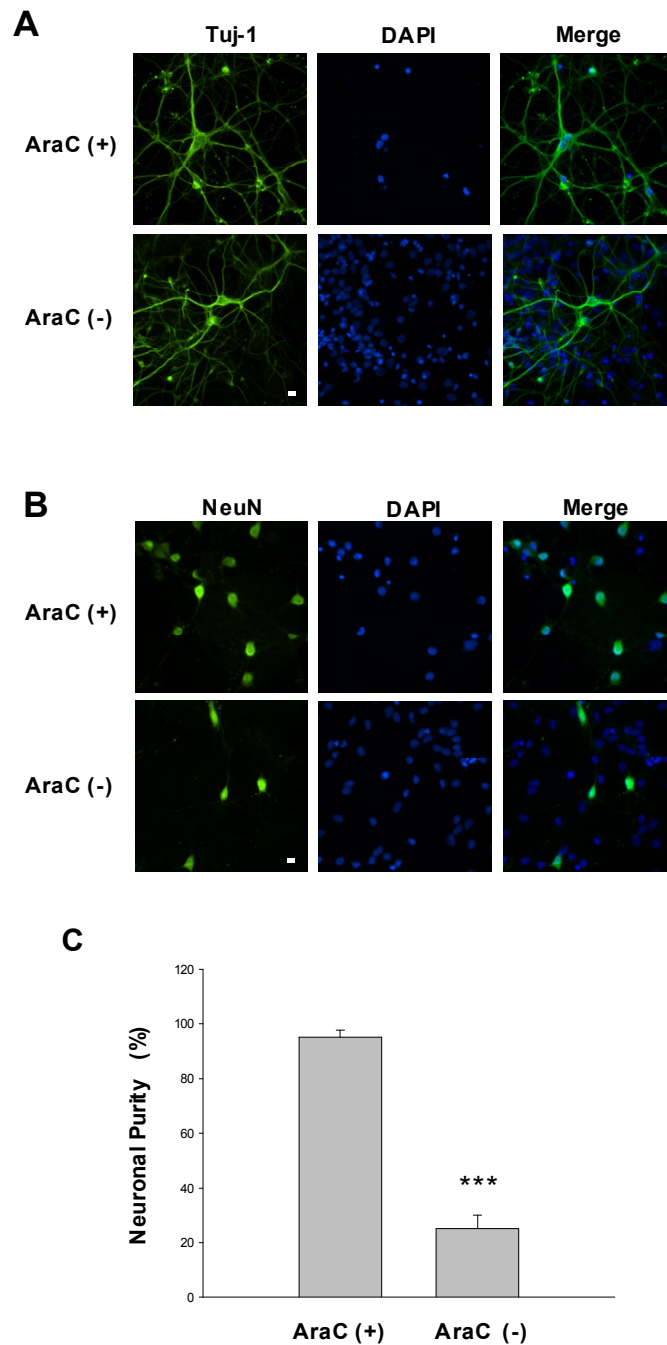


Fig. 8. Neuronal purity in primary cortical neuron cultures. Cultures were treated with 1 μ M arabinofuranosyl cytidine (Ara-C) to prevent glial proliferation at 4th days. A-B. Cultured primary cortical neurons were marked with Tuj-1 and NeuN by immunofluorescence. C. Quantification of Ara-C positive cell and negative cell. Blue colors show nuclei stained with DAPI and green colors show the fluorescence of Tuj-1 and NeuN. Scale bar, 10 μ m.

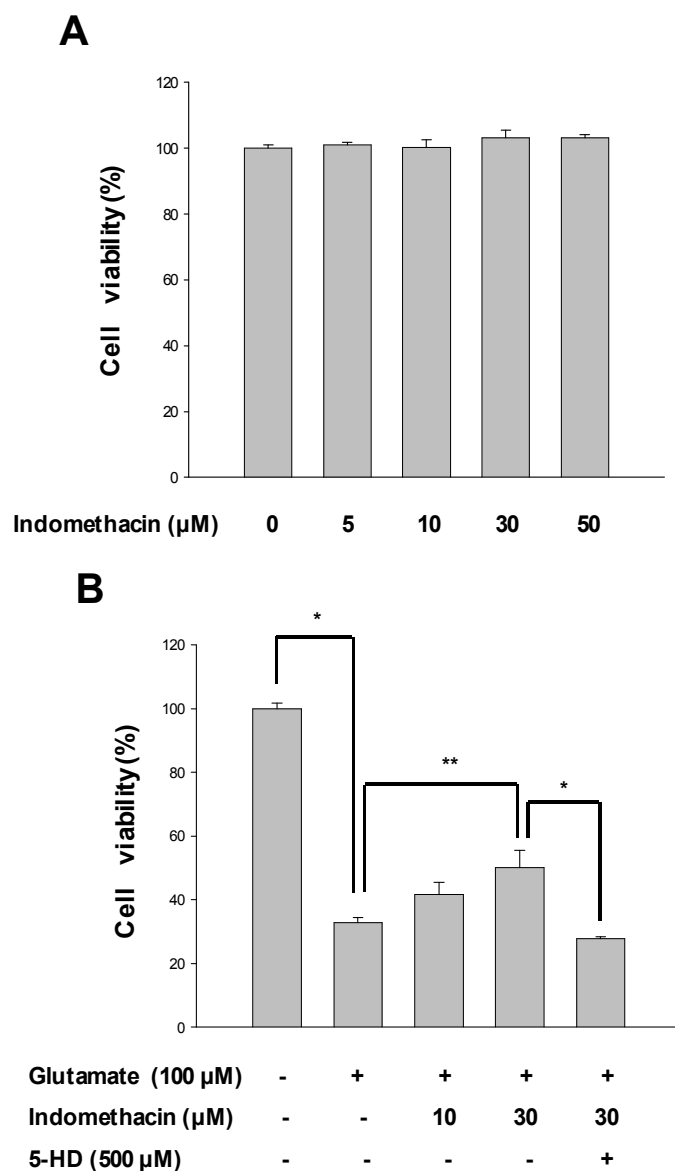


Fig. 9. Effects of indomethacin and 5HD on glutamate-induced neuronal toxicity.

A. Cytotoxicity of indomethacin was evaluated by MTT assay. B. Primary cortical neurons were treated with glutamate (100 μM) for 30 min in the presence or absence of indomethacin (10 and 30 μM). Indomethacin was pretreated for 5 min before glutamate stimulation. The neuroprotective effects of indomethacin were evaluated by using MTT cell viability assays. Groups were compared by % of untreated control group. #, $p < 0.05$ as compared to the untreated controls and *, $p < 0.05$ as compared to the group treated with glutamate alone.

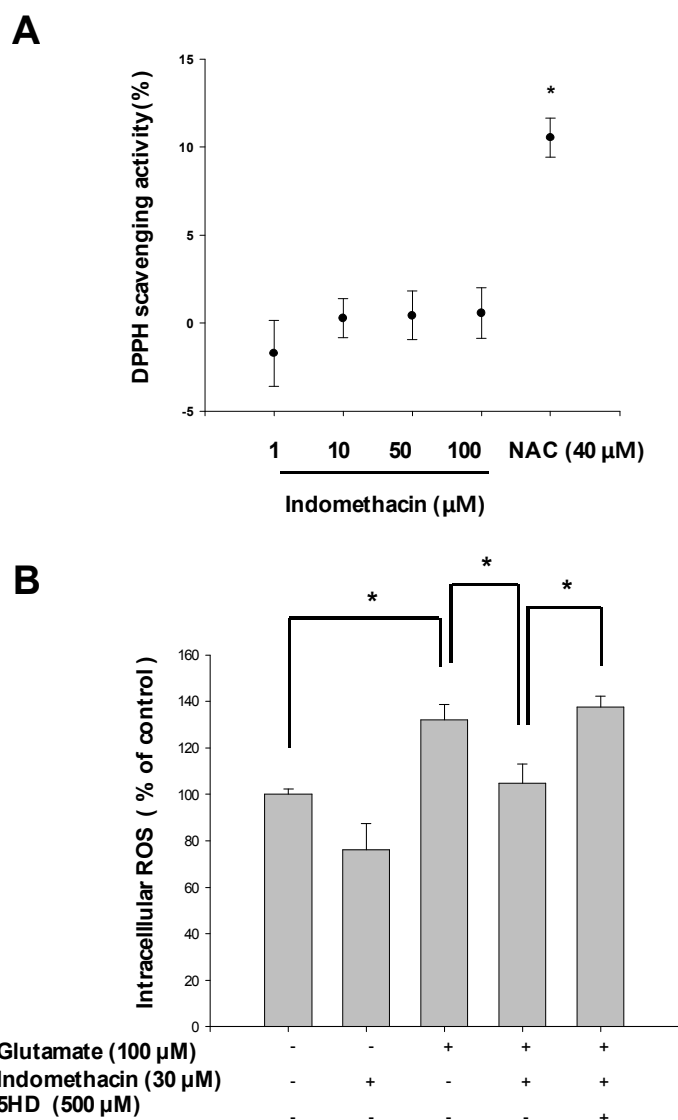


Fig. 10. Anti-oxidant activities of indomethacin.

A. Various concentrations (1, 10, 50 and 100 μM) of indomethacin were incubated for 2 h with DPPH and the amounts of DPPH radicals were spectrophotometrically determined. B. Primary cortical neurons were treated with glutamate (100 μM) for 30 min to induce neuronal cell death. Indomethacin (30 μM) in the presence or absence of 5HD (500 μM) was pretreated for 5 min before glutamate stimulation. Then intracellular ROS levels were detected by using a spectrofluorometer using DCF-DA.

*, $p < 0.05$ as compared to the indicated group.

3.4. Effect of indomethacin on the mitochondrial membrane potential, cytosol calcium and mitochondrial calcium

Raising evidence indicates that many agents showing neuroprotective effects via the modulation of mitochondrial calcium concentrations (Hung *et al.*, 2010). Calcium homeostasis and dissipation of mitochondrial membrane potential is a critical event in the process of apoptosis. To evaluate the exact neuroprotective mechanism of indomethacin, we investigated that the effect of indomethacin on the mitochondrial membrane potential, cytosol calcium and mitochondrial calcium by real-time recording. TMRE, which is sequestered by mitochondria in proportion to $\Delta\Psi_m$ and the decrease in TMRE fluorescence intensities reflects mitochondrial depolarization. TMRM fluorescence values from individual cells were normalized to the value before drug treatment. Traces shown in Fig. 11-A show average recordings of TMRM fluorescence intensities obtained from individual cells. Indomethacin induced the dose (1, 10 and 30 μM)-dependent decrease in TMRE fluorescence intensities, indicating that indomethacin is capable of inducing mitochondrial depolarization. Treatments of various concentrations of indomethacin (10, 30 and 50 μM) did not induce cytosol or mitochondrial calcium increases.

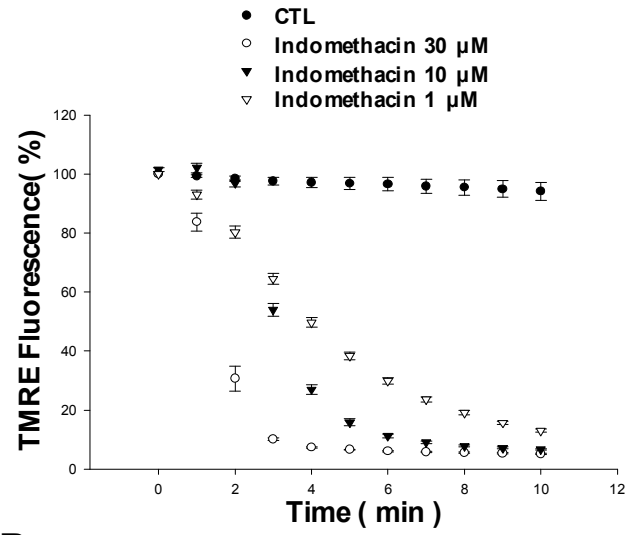
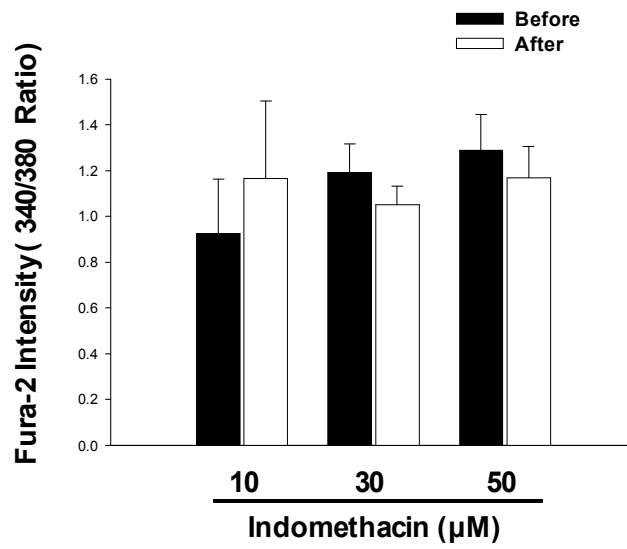
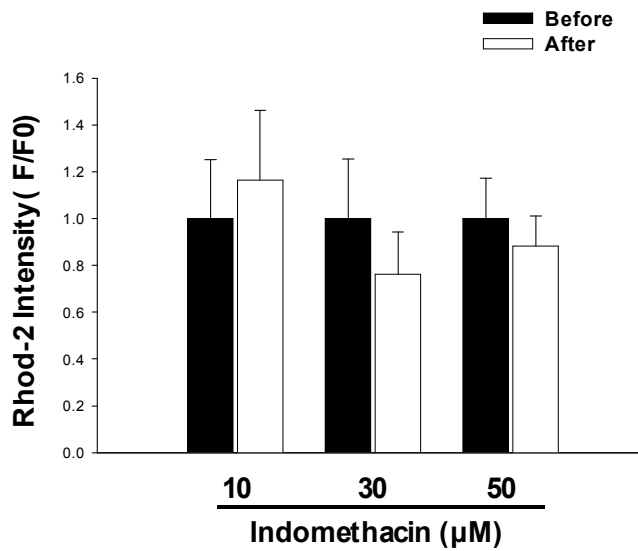
A**B****C**

Fig. 11. Effect of indomethacin on the mitochondrial membrane potential, cytosol calcium and mitochondrial calcium.

A. Real-time measurement of $\Delta\Psi_m$ was conducted with MetaFluor software by using a cationic fluorescent probe TMRE. Various concentrations of indomethacin (1, 10 and 30 μM) were superfused in a recording chamber and TMRE fluorescence values from individual cells were normalized to the value at starting point of drug treatment. Traces show average recordings of TMRE fluorescence intensities. B. Dual recording of cytosolic calcium and mitochondrial calcium. Cultured neurons were loaded for 45 min in the cell culture medium at 37°C with Fura-2 AM (5 μM) and Pluronic F127 (0.1%) and after that transfer to Rhod-2 AM (2 μM) at 4°C for 30 min. Various concentrations of indomethacin (10, 30 and 50 μM) were superfused in a recording chamber and fluorescence values from individual cells were recorded by using real time imaging system. Quantifications of cytosolic calcium and mitochondrial calcium alteration at 1 min-time point after drug treatment were compared among different groups.

3.5. Mitochondrial K_{ATP} channel blockade abolishes neuroprotective effect of indomethacin on mitochondrial membrane potential

In next study, we evaluated whether mito K_{ATP} channels regulate mitochondria depolarization which was induced by indomethacin. Treatment of 5HD, a specific mito K_{ATP} channels blocker, significantly decreased mitochondrial depolarization which was induced by indomethacin (Fig. 12-A). Primary cortical neurons were treated with indomethacin (30 μ M) for 10 min in the presence or absence of 5HD (500 μ M) and the reduction of TMRE fluorescence at 10 min time point was $14.8 \pm 1.5\%$ and $5.1 \pm 0.1\%$ respectively (Fig. 12-B).

3.6. Mitochondrial K_{ATP} channel blockade abolishes neuroprotective effect of indomethacin on glutamate-induced mitochondrial superoxide generation

Many previous studies indicates that ROS plays a major role in the pathogenesis of neurodegenerative disorders (Bernardi *et al.*, 1999) and also in excitotoxic cell death models (Dykens *et al.*, 1987). Mitochondria are significant sources of ROS and the primary ROS made by mitochondria is superoxide ($O_2^{\cdot-}$), which is sequentially converted to H_2O_2 by the enzyme superoxide dismutase (SOD). The main source of $O_2^{\cdot-}$ in mitochondria is the complex III (Muller *et al.*, 2003) (St-Pierre *et al.*, 2002) (Turrens, 1997) and complex IV (Mailier, 1990) in mitochondrial electron transport chain. In the next set of experiment we investigated the effect of indomethacin and 5HD on glutamate-induced superoxide generation by real-time recording. MitoSOX Red, which was a mitochondria specific superoxide indicator permeates live cells and selectively targets mitochondria. It is rapidly oxidized by superoxide but not by other ROS or reactive nitrogen species (RNS). The relative fluorescence intensity data from real-time recording revealed that indomethacin treatment (30 μ M) significantly attenuated the intracellular superoxide levels (Fig 13) in

glutamate (100 μ M, 30 min)-stimulated neurons and 5HD treatment abolished the inhibitory effect of indomethacin on glutamate-induced superoxide generation.

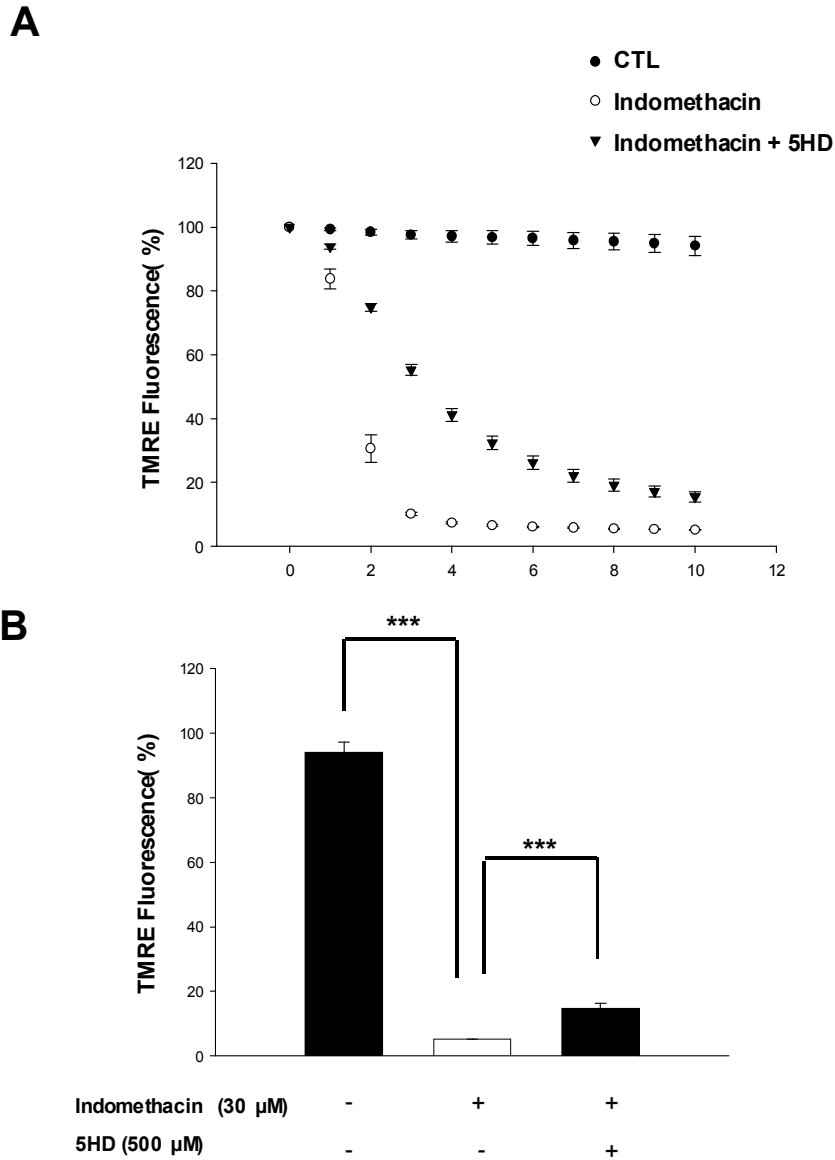


Fig. 12. Inhibitory effect of 5HD on indomethacin-induced mitochondrial depolarization. A. Real-time measurement of $\Delta\Psi_m$ was conducted with MetaFluor software by using a cationic fluorescent probe TMRE. Indomethacin (30 μ M) in the presence or absence of 5HD (500 μ M) were superfused in a recording chamber and TMRE fluorescence values from individual cells were normalized to the value at starting point of drug treatment. Traces show the averaged recordings of TMRE fluorescence intensities. B. Quantification of TMRE at 10 min-time point after drug treatment was compared among different group.

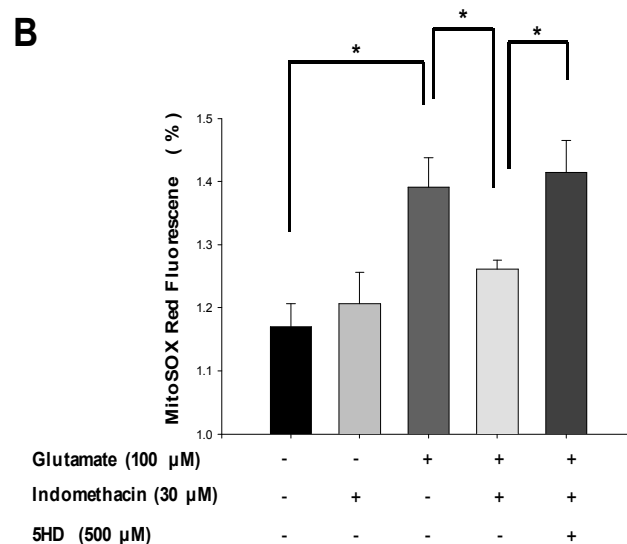
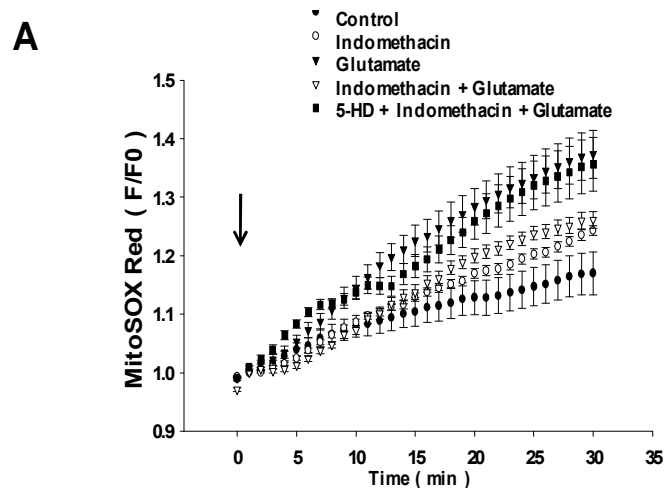


Fig. 13. Effects of indomethacin and 5HD on glutamate-induced mitochondrial superoxide generation. A. Real-time measurement of mitochondrial superoxide generation was conducted by real-time recording using a cationic fluorescent probe MitoSOX Red. Indicated agents were superfused in recording chamber and MitoSOX Red fluorescence values from individual cells were normalized to the value at starting point of drug treatment. Indomethacin (30 μ M) in the presence or absence of 5HD (500 μ M) was pretreated for 5 min before glutamate stimulation. Traces show the averaged recordings of TMRE fluorescence intensities. B. Quantification of MitoSOX Red at 30 min-time point after drug treatment was compared among different groups.

3.7. Mitochondrial K_{ATP} channel blockade abolishes neuroprotective effect of indomethacin on glutamate-induced mitochondrial calcium overload

Calcium signaling is essential for life processes including neuronal excitability, synaptic plasticity, gene transcription and apoptosis (Berridge et al., 1998). Excessive mitochondrial calcium overload leads to mitochondrial permeability transition pore opening and induction of apoptosis. Therefore, we investigated the regulatory effect of indomethacin (30 μ M) on mitochondrial Ca^{2+} deregulation in glutamate (100 μ M, 30 min)-induced neuronal neurotoxicity. Real-time recording of mitochondrial calcium was accomplished by using Rhod-2 AM fluorescent indicators for mitochondrial calcium. The AM ester forms of these Rhod-2 indicators are cationic, resulting in potential-driven uptake into mitochondria. This has led to the use of rhod-2 as a selective indicator for mitochondrial calcium (Babcock et al., 1997; Hajnoczky et al., 1995). Glutamate treatment remarkably increased mitochondrial Ca^{2+} levels and this increases in mitochondrial Ca^{2+} levels were significantly attenuated by indomethacin treatment (Fig. 14). Furthermore, 5HD treatment abolished the inhibitory effect of indomethacin.

3.8. Mitochondrial K_{ATP} channel blockade abolishes neuroprotective effect of indomethacin on glutamate-induced mPTP opening

Mitochondrial calcium overload may promote opening of the mPTP and the intrinsic pathway to apoptosis. Therefore in the last step of this study, we examined the role of indomethacin and 5HD in glutamate-induced mPTP opening using calcein- $CoCl_2$ method. Opening of mPTP promotes mitochondrial calcein quenching. Under resting condition, calcein fluorescence was largely intact and colocalized with the potential-sensitive mitochondrial marker, MitoTracker Red CMXRos. Indomethacin treatment significantly

decreased calcein quenching in glutamate (100 μ M, 30 min)-stimulated neurons and 5HD treatment abolished the inhibitory effect of indomethacin on glutamate-induced calcein quenching (Fig 15).

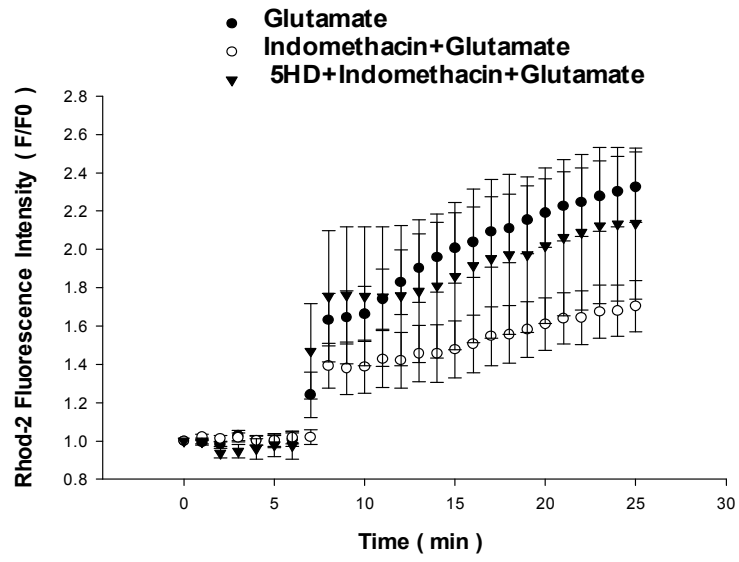
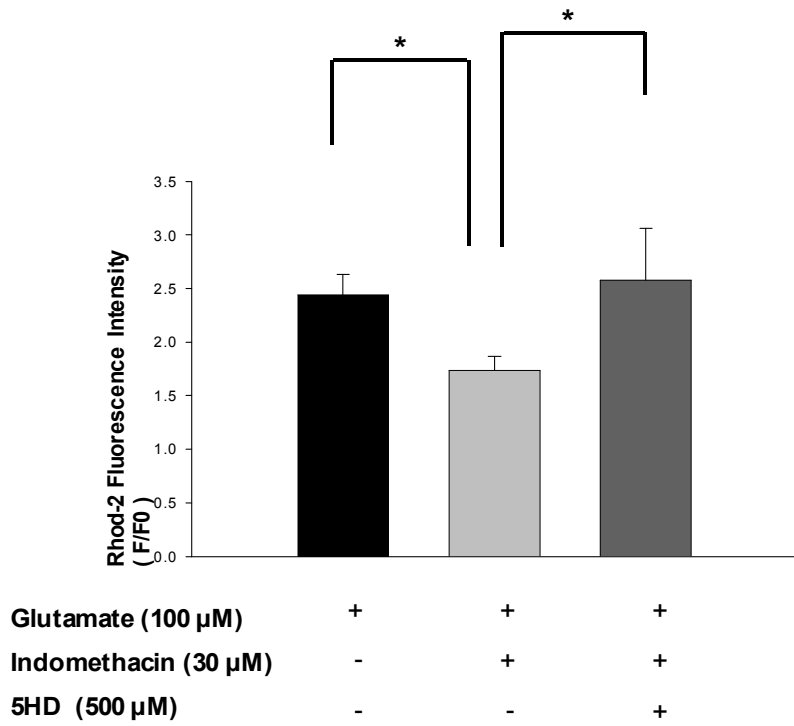
A**B**

Fig. 14. Effects of indomethacin and 5HD on glutamate-induced mitochondrial mitochondrial calcium overload. A. Real-time measurement of mitochondrial calcium was conducted by real-time recording using a cationic fluorescent probe Rhod-2 AM. Indicated agents were superfused in recording chamber and Rhod-2 fluorescence values from individual cells were normalized to the value at starting point of drug treatment. Indomethacin (30 μM) in the presence or absence of 5HD (500 μM) was pretreated for 5 min before glutamate stimulation. Traces show the averaged recordings of Rhod-2 fluorescence intensities. B. Quantification of Rhod-2 fluorescence intensities at 25 min-time point after drug treatment were compared among different groups.

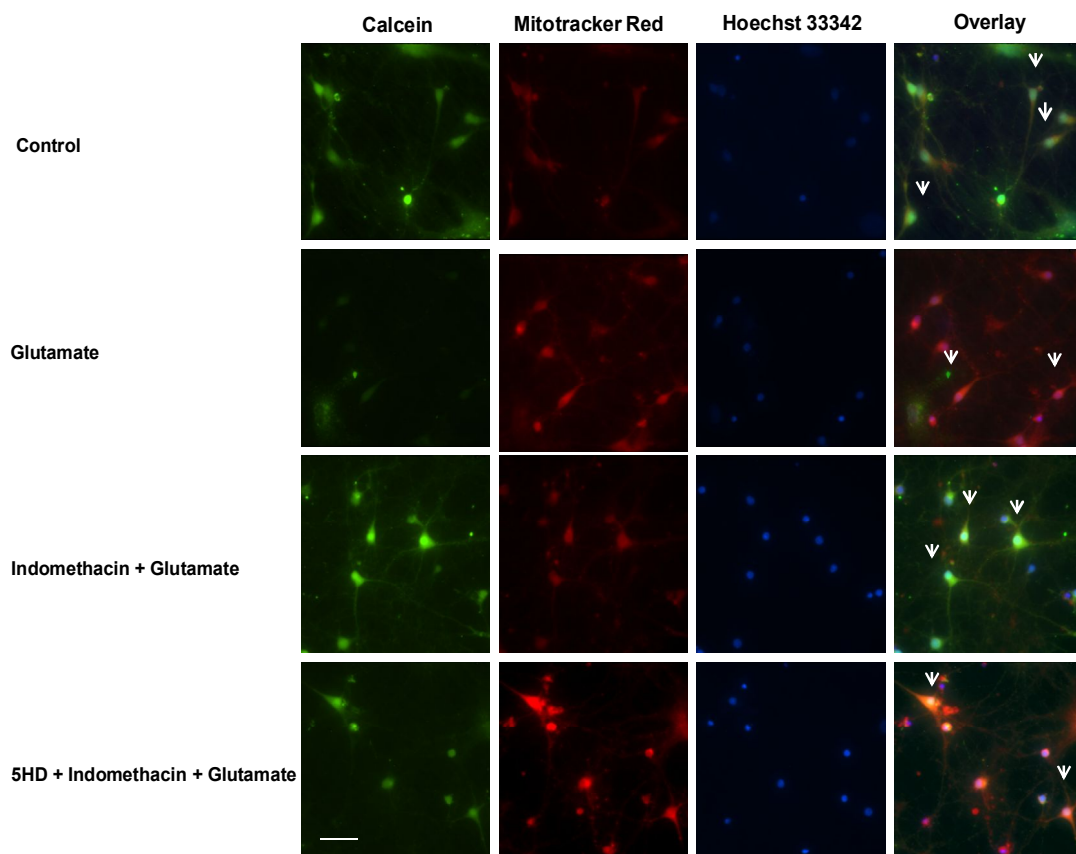


Fig. 15. Effects of indomethacin and 5HD on glutamate-induced mPTP opening.

Mitochondrial permeability transition pore (mPTP) opening was assessed directly by the calcein/CoCl₂ method. Primary cortical neurons were stimulated by glutamate (100 μM) for 30 min. Indomethacin (30 μM) in the presence or absence of 5HD (500 μM) was pretreated for 5 min before glutamate stimulation. After treatment neurons were loaded with calcein-AM (1 μM), CoCl₂ (1 mM) and MitoTracker Red CMXRos (200 nM) for 15min at 37°C. Quenching of calcein fluorescence indicates opening of mPTP. Scale bar, 100 μm.

4. Discussion

Glutamate is the major excitatory neurotransmitter in the central nervous system to regulate neuronal metabolism and gene expression which was necessary for brain development. But overstimulation of NMDA receptors by excess glutamate release from presynaptic cells induces cell death in a process known as excitotoxicity and mitochondrial calcium overload is closely associated with this process. $\Delta\Psi_m$ contributes to determining a driving force for Ca^{2+} to enter the mitochondria via Ca^{2+} -permeable channels such as the mitochondrial Ca^{2+} uniporter (Kirichok *et al.*, 2004) and ATP synthesis.

In physiological condition, mitochondrial membrane potential ranges -120 to -180 mV, which is more negative than that of plasma membrane (Hung *et al.*, 2010) (Kroemer *et al.*, 2007). It is also an important factor in the maintenance of mitochondrial homeostasis: both mitochondrial calcium uptake (White and Reynolds, 1997) and production of ROS. Physiological mitochondrial ROS which was a product of respiration is important for cell signaling (Brookes and Darley-Usmar, 2002) (Brookes *et al.*, 2002) but a burst of ROS may induce mPTP opening (Green and Reed, 1998) (Grijalba *et al.*, 1999). Some studies showed (Brookes and Darley-Usmar, 2004) that PT pore triggering by ROS is potentiated by calcium and indicated a hypothesis that the combination of calcium plus a pathological stimulus such as ROS can elicit mitochondrial dysfunction (Brookes *et al.*, 2004). But it is still unclear whether ROS generation is just a consequence of mPTP opening and cytochrome *c* release or an integral part of the signaling machinery of mPTP opening.

Many ions, nucleotides and proteins traverse the mitochondrial membranes in tightly regulated mitochondrial membrane potential. 1) Mitochondrial Ca^{2+} regulation channels. Ca^{2+} accumulation into mitochondria occurs via mitochondrial calcium uniporter (MCU) and

mitochondrial ryanodine receptor (mRyR). And extrusion of mitochondrial Ca^{2+} is regulated by $\text{Na}^+/\text{Ca}^{2+}$ exchange (mNCX), which is coupled to the H^+ gradient through Na^+/H^+ ATP ase (Szabadkai and Duchen, 2008). 2) Mitochondrial K^+ channels. Different types of potassium channels have been described in the inner mitochondrial membrane. The ATP-regulated potassium channel (mitK_{ATP} channel) which is inactivated by ATP; The large Ca^{2+} -activated potassium channel (mitBK_{Ca} channel), which was activated by changes of membrane potential or intracellular Ca^{2+} (Szewczyk *et al.*, 2010) and blocked by charybdotoxin (ChTx) or iberiotoxin (IbTx); The margatoxin-sensitive K_v1.3 potassium channel (mitK_v1.3 channel), which was voltage-sensitive was identified in the inner mitochondrial membrane of lymphocytes (Choma *et al.*, 2009). 3) K^+/H^+ ATP ase, which removes K^+ using the proton gradient.

K_{ATP} channels are found in many locations within cells, including the plasma membrane and the inner mitochondrial membrane. And it is reported that there were 7-fold more mitoK_{ATP} channels in neuron when compared with mitochondria in cardiac tissues, indicating an important role for these channels in neurons (Bernardi *et al.*, 1999) (Nakagawa *et al.*, 2012).

The principal findings of this study are as follow. 1) Indomethacin, which induce mitochondrial membrane depolarization but has no antioxidant activity, significantly inhibited the neuronal cell death induced by glutamate. 2) Indomethacin prevented the increase mitochondrial superoxide generation, mitochondrial calcium overload and mPTP pore opening induced by glutamate stimulation. These effects were abolished by 5HD, a specific mitK_{ATP} channel antagonist. Our findings suggest that the possible activation of mitoK_{ATP} channels by indomethacin may prevent mitochondrial from mitochondrial calcium overload, precluding ROS production or suppressing cytochrome c release to prevent neuronal cell death.

In conclusion, indomethacin protects neurons against glutamate excitotoxicity via regulating mitK_{ATP} channel and mitK_{ATP} channel could be a key target in neuronal cell death

via handling mitochondrial calcium.

Reference

1. Babcock DF, Herrington J, Goodwin PC, Park YB and Hille B. 1997. Mitochondrial participation in the intracellular Ca²⁺ network. *J Cell Biol* **136**: 833-844.
2. Bajgar R, Seetharaman S, Kowaltowski AJ, Garlid KD and Paucek P. 2001. Identification and properties of a novel intracellular (mitochondrial) ATP-sensitive potassium channel in brain. *J Biol Chem* **276**: 33369-33374.
3. Bernardi P, Scorrano L, Colonna R, Petronilli V and Di Lisa F. 1999. Mitochondria and cell death. Mechanistic aspects and methodological issues. *Eur J Biochem* **264**: 687-701.
4. Berridge MJ, Bootman MD and Lipp P. 1998. Calcium--a life and death signal. *Nature* **395**: 645-648.
5. Breyer A, Elstner M, Gillessen T, Weiser D and Elstner E. 2007. Glutamate-induced cell death in neuronal HT22 cells is attenuated by extracts from St. John's wort (*Hypericum perforatum* L.). *Phytomedicine* **14**: 250-255.
6. Brookes P and Darley-Usmar VM. 2002. Hypothesis: the mitochondrial NO(*) signaling pathway, and the transduction of nitrosative to oxidative cell signals: an alternative function for cytochrome C oxidase. *Free Radic Biol Med* **32**: 370-374.
7. Brookes PS and Darley-Usmar VM. 2004. Role of calcium and superoxide dismutase in sensitizing mitochondria to peroxynitrite-induced permeability transition. *Am J Physiol Heart Circ Physiol* **286**: H39-46.
8. Brookes PS, Levonen AL, Shiva S, Sarti P and Darley-Usmar VM. 2002. Mitochondria: regulators of signal transduction by reactive oxygen and nitrogen species. *Free Radic Biol Med* **33**: 755-764.
9. Brookes PS, Yoon Y, Robotham JL, Anders MW and Sheu SS. 2004. Calcium, ATP, and ROS: a mitochondrial love-hate triangle. *Am J Physiol Cell Physiol* **287**: C817-833.
10. Busija DW, Lacza Z, Rajapakse N, Shimizu K, Kis B, Bari F, Domoki F and Horiguchi T.

2004. Targeting mitochondrial ATP-sensitive potassium channels--a novel approach to neuroprotection. *Brain Res Brain Res Rev* **46**: 282-294.
- 11.** Choi SY, Ko HC, Ko SY, Hwang JH, Park JG, Kang SH, Han SH, Yun SH and Kim SJ. 2007. Correlation between flavonoid content and the NO production inhibitory activity of peel extracts from various citrus fruits. *Biol Pharm Bull* **30**: 772-778.
- 12.** Choma K, Bednarczyk P, Koszela-Piotrowska I, Kulawiak B, Kudin A, Kunz WS, Dolowy K and Szewczyk A. 2009. Single channel studies of the ATP-regulated potassium channel in brain mitochondria. *J Bioenerg Biomembr* **41**: 323-334.
- 13.** Clapham DE. 1995. Calcium signaling. *Cell* **80**: 259-268.
- 14.** Clapham DE. 2007. Calcium signaling. *Cell* **131**: 1047-1058.
- 15.** Crompton M. 1999. The mitochondrial permeability transition pore and its role in cell death. *Biochem J* **341 (Pt 2)**: 233-249.
- 16.** Cui Y, Wu J, Jung SC, Park DB, Maeng YH, Hong JY, Kim SJ, Lee SR, Kim SJ, Kim SJ and Eun SY. 2010. Anti-neuroinflammatory Activity of Nobiletin on Suppression of Microglial Activation. *Biol Pharm Bull* **33**: 1814-1821.
- 17.** Dykens JA, Stern A and Trenkner E. 1987. Mechanism of kainate toxicity to cerebellar neurons in vitro is analogous to reperfusion tissue injury. *J Neurochem* **49**: 1222-1228.
- 18.** Feissner RF, Skalska J, Gaum WE and Sheu SS. 2009. Crosstalk signaling between mitochondrial Ca²⁺ and ROS. *Front Biosci* **14**: 1197-1218.
- 19.** Galati EM, Monforte MT, Kirjavainen S, Forestieri AM, Trovato A and Tripodo MM. 1994. Biological effects of hesperidin, a citrus flavonoid. (Note I): antiinflammatory and analgesic activity. *Farmacologia* **40**: 709-712.
- 20.** Garcia-Martinez EM, Sanz-Blasco S, Karachitos A, Bandez MJ, Fernandez-Gomez FJ, Perez-Alvarez S, de Mera RM, Jordan MJ, Aguirre N, Galindo MF, Villalobos C, Navarro A, Kmita H and Jordan J. 2010. Mitochondria and calcium flux as targets of neuroprotection caused by minocycline in cerebellar granule cells. *Biochem Pharmacol* **79**: 239-250.

21. Garlid KD, Dos Santos P, Xie ZJ, Costa AD and Paucek P. 2003. Mitochondrial potassium transport: the role of the mitochondrial ATP-sensitive K(+) channel in cardiac function and cardioprotection. *Biochim Biophys Acta* **1606**: 1-21.
22. Green DR and Reed JC. 1998. Mitochondria and apoptosis. *Science* **281**: 1309-1312.
23. Grijalba MT, Vercesi AE and Schreier S. 1999. Ca²⁺-induced increased lipid packing and domain formation in submitochondrial particles. A possible early step in the mechanism of Ca²⁺-stimulated generation of reactive oxygen species by the respiratory chain. *Biochemistry* **38**: 13279-13287.
24. Hajnoczky G, Robb-Gaspers LD, Seitz MB and Thomas AP. 1995. Decoding of cytosolic calcium oscillations in the mitochondria. *Cell* **82**: 415-424.
25. Hung CH, Ho YS and Chang RC. 2010. Modulation of mitochondrial calcium as a pharmacological target for Alzheimer's disease. *Ageing Res Rev* **9**: 447-456.
26. Inoue I, Nagase H, Kishi K and Higuti T. 1991. ATP-sensitive K⁺ channel in the mitochondrial inner membrane. *Nature* **352**: 244-247.
27. Ishimura A, Ishige K, Taira T, Shimba S, Ono S, Ariga H, Tezuka M and Ito Y. 2008. Comparative study of hydrogen peroxide- and 4-hydroxy-2-nonenal-induced cell death in HT22 cells. *Neurochem Int* **52**: 776-785.
28. Jouaville LS, Pinton P, Bastianutto C, Rutter GA and Rizzuto R. 1999. Regulation of mitochondrial ATP synthesis by calcium: evidence for a long-term metabolic priming. *Proc Natl Acad Sci U S A* **96**: 13807-13812.
29. Kirichok Y, Krapivinsky G and Clapham DE. 2004. The mitochondrial calcium uniporter is a highly selective ion channel. *Nature* **427**: 360-364.
30. Ko H-C, Jang M-G, Kang C-H, Lee N-H, Kang S-I, Lee S-R, Park D-B and Kim S-J. 2010. Preparation of a polymethoxyflavone-rich fraction (PRF) of *Citrus sunki* Hort. ex Tanaka and its antiproliferative effects. *Food Chemistry* **123**: 484-488.
31. Kroemer G, Galluzzi L and Brenner C. 2007. Mitochondrial membrane permeabilization in cell death. *Physiol Rev* **87**: 99-163.

32. Lasorsa FM, Pinton P, Palmieri L, Fiermonte G, Rizzuto R and Palmieri F. 2003. Recombinant expression of the Ca(2+)-sensitive aspartate/glutamate carrier increases mitochondrial ATP production in agonist-stimulated Chinese hamster ovary cells. *J Biol Chem* **278**: 38686-38692.
33. Lee CH, Jeong TS, Choi YK, Hyun BH, Oh GT, Kim EH, Kim JR, Han JI and Bok SH. 2001. Anti-atherogenic effect of citrus flavonoids, naringin and naringenin, associated with hepatic ACAT and aortic VCAM-1 and MCP-1 in high cholesterol-fed rabbits. *Biochem Biophys Res Commun* **284**: 681-688.
34. Li S, Pan M-H, Lo C-Y, Tan D, Wang Y, Shahidi F and Ho C-T. 2009. Chemistry and health effects of polymethoxyflavones and hydroxylated polymethoxyflavones. *Journal of Functional Foods* **1**: 2-12.
35. Liu Y, Sato T, Seharaseyon J, Szewczyk A, O'Rourke B and Marban E. 1999. Mitochondrial ATP-dependent potassium channels. Viable candidate effectors of ischemic preconditioning. *Ann NY Acad Sci* **874**: 27-37.
36. Lundholm K, Gelin J, Hyltander A, Lonroth C, Sandstrom R, Svaninger G, Korner U, Gulich M, Karrefors I, Norli B and et al. 1994. Anti-inflammatory treatment may prolong survival in undernourished patients with metastatic solid tumors. *Cancer Res* **54**: 5602-5606.
37. Mailer K. 1990. Superoxide radical as electron donor for oxidative phosphorylation of ADP. *Biochem Biophys Res Commun* **170**: 59-64.
38. Misra HP and Fridovich I. 1972. The role of superoxide anion in the autoxidation of epinephrine and a simple assay for superoxide dismutase. *J Biol Chem* **247**: 3170-3175.
39. Muller FL, Roberts AG, Bowman MK and Kramer DM. 2003. Architecture of the Qo site of the cytochrome bc1 complex probed by superoxide production. *Biochemistry* **42**: 6493-6499.
40. Nakagawa I, Wajima D, Tamura K, Nishimura F, Park YS and Nakase H. 2012. The neuroprotective effect of diazoxide is mediated by mitochondrial ATP-dependent

- potassium channels in a rat model of acute subdural hematoma. *J Clin Neurosci* **20**: 144-147.
41. Nunez L, Valero RA, Senovilla L, Sanz-Blasco S, Garcia-Sancho J and Villalobos C. 2006. Cell proliferation depends on mitochondrial Ca^{2+} uptake: inhibition by salicylate. *J Physiol* **571**: 57-73.
42. Onozuka H, Nakajima A, Matsuzaki K, Shin RW, Ogino K, Saigusa D, Tetsu N, Yokosuka A, Sashida Y, Mimaki Y, Yamakuni T and Ohizumi Y. 2008. Nobiletin, a citrus flavonoid, improves memory impairment and Abeta pathology in a transgenic mouse model of Alzheimer's disease. *J Pharmacol Exp Ther* **326**: 739-744.
43. Pinton P, Giorgi C, Siviero R, Zecchini E and Rizzuto R. 2008. Calcium and apoptosis: ER-mitochondria Ca^{2+} transfer in the control of apoptosis. *Oncogene* **27**: 6407-6418.
44. Pizzo P, Drago I, Filadi R and Pozzan T. 2012. Mitochondrial Ca^{2+} homeostasis: mechanism, role, and tissue specificities. *Pflugers Arch* **464**: 3-17.
45. Rizzuto R, Marchi S, Bonora M, Aguiari P, Bononi A, De Stefani D, Giorgi C, Leo S, Rimessi A, Siviero R, Zecchini E and Pinton P. 2009. Ca^{2+} transfer from the ER to mitochondria: when, how and why. *Biochim Biophys Acta* **1787**: 1342-1351.
46. Salvioli S, Ardizzoni A, Franceschi C and Cossarizza A. 1997. JC-1, but not DiOC6(3) or rhodamine 123, is a reliable fluorescent probe to assess delta psi changes in intact cells: implications for studies on mitochondrial functionality during apoptosis. *FEBS Lett* **411**: 77-82.
47. Sanz-Blasco S, Valero RA, Rodriguez-Crespo I, Villalobos C and Nunez L. 2008. Mitochondrial Ca^{2+} overload underlies Abeta oligomers neurotoxicity providing an unexpected mechanism of neuroprotection by NSAIDs. *PLoS One* **3**: e2718.
48. Scaduto RC, Jr. and Grotyohann LW. 1999. Measurement of mitochondrial membrane potential using fluorescent rhodamine derivatives. *Biophys J* **76**: 469-477.
49. St-Pierre J, Buckingham JA, Roebuck SJ and Brand MD. 2002. Topology of superoxide production from different sites in the mitochondrial electron transport chain. *J Biol Chem*

277: 44784-44790.

50. Storozhevych TP, Senilova YE, Brustovetsky T, Pinelis VG and Brustovetsky N. 2010. Neuroprotective effect of KB-R7943 against glutamate excitotoxicity is related to mild mitochondrial depolarization. *Neurochem Res* **35**: 323-335.
51. Szabadkai G and Duchen MR. 2008. Mitochondria: the hub of cellular Ca²⁺ signaling. *Physiology (Bethesda)* **23**: 84-94.
52. Szewczyk A, Kajma A, Malinska D, Wrzosek A, Bednarczyk P, Zablocka B and Dolowy K. 2010. Pharmacology of mitochondrial potassium channels: dark side of the field. *FEBS Lett* **584**: 2063-2069.
53. Turrens JF. 1997. Superoxide production by the mitochondrial respiratory chain. *Biosci Rep* **17**: 3-8.
54. Valero RA, Senovilla L, Nunez L and Villalobos C. 2008. The role of mitochondrial potential in control of calcium signals involved in cell proliferation. *Cell Calcium* **44**: 259-269.
55. Wang XQ, Xiao AY, Sheline C, Hyrc K, Yang A, Goldberg MP, Choi DW and Yu SP. 2003. Apoptotic insults impair Na⁺, K⁺-ATPase activity as a mechanism of neuronal death mediated by concurrent ATP deficiency and oxidant stress. *J Cell Sci* **116**: 2099-2110.
56. White RJ and Reynolds IJ. 1997. Mitochondria accumulate Ca²⁺ following intense glutamate stimulation of cultured rat forebrain neurones. *J Physiol* **498 (Pt 1)**: 31-47.

ABSTRACT IN KOREAN

미토콘드리아 막전압은 세포 내 칼슘이 미토콘드리아로 유입하는 과정에서 중요한 조절인자로서 작용한다. 최근 연구결과에 의하면 미토콘드리아 탈분극은 미토콘드리아 칼슘 과부하의 조절을 통하여 신경 세포의 사멸을 억제할 수 있는 신경 보호작용의 새로운 기전으로 평가될 수 있다. 진굴 과피에 있는 많은 활성화합물질들은 항염작용 및 항산화작용을 포함한 많은 생물학적 활성이 있는 것으로 조사되었다. 연구결과에 의하면 활성화합물질들이 뇌 퇴행성질환 모델에서의 신경보호효과는 조사되었지만 그 정확한 메커니즘은 아직 규명되지 않았다. 하여 본 연구에서는 산화적 신경 독성에 대한 진굴 과피 에탄올추출물의 신경보호효과와 그 작용기전을 확인하였다. 실험결과 CPE 를 처리하였을 때 산화 신경 독성 모델로 사용된 H_2O_2 를 처리한 HT-22 신경세포 손상사멸이 현저하게 억제되는 것을 확인하였다. 또한 CPE 는 강력한 라디칼 소거작용을 통한 항산화작용 뿐만 아니라 H_2O_2 에 의한 세포질과 미토콘드리아 칼슘 증가와 이로 인한 신경세포 사멸이 억제되는 것을 확인하였다. 또한 본 연구에서는 nobiletin 과 같은 CPE 의 활성화합물질들이 미토콘드리아 막전압을 탈분극 시키는 것을 확인하였다. 이는 CPE 의 신경보호효과는 항산화작용 뿐만 아니라 미토콘드리아

막전압을 탈분극 시키는 것을 통하여 세포사멸을 일으키는 미토콘드리아 칼슘 과부하를 억제하는 두 가지 작용기전을 통하여 작용하는 것으로 시사된다.

다음 연구에서는 항산화작용 기전을 제외한 미토콘드리아 탈분극을 통한 신경보호작용만 조사하기 위하여 항산화작용이 없는 항염제의 하나인 indomethacin 을 선택하여 조사를 진행하였다. 실험결과 primary cortical neuron 의 glutamate 를 이용한 흥분독성모델에서 indomethacin 은 현저한 신경보호작용이 있는 것으로 확인되었고 이는 미토콘드리아 K_{ATP} 채널의 specific antagonist 인 5HD 를 처리하였을 때 다시 억제되는 것을 확인하였다. 또한 5HD 는 indomethacin 의 탈분극 작용을 억제할 뿐만 아니라 glutamate 에 의한 미토콘드리아 칼슘 과부하와 이로 인한 superoxide 의 증가, mPTP opening 을 억제하는 indomethacin 의 작용들을 모두 억제하는 것으로 확인되었다.

결론적으로 CPE 와 indomethacin 은 미토콘드리아 탈분극 기전을 통하여 신경보호작용을 하는 새로운 agent 들로 시사되고 미토콘드리아 K_{ATP} 채널과 같은 미토콘드리아 이온 채널들이 새로운 신경보호의 치료 전략으로의 활용가능성을 시사하고 있다.

감사의 글

처음 제주에 온지가 엇그제 같은데 벌써 6년이 지나갔습니다. 지금 6년의 학위과정을 돌아보면 많은 도움과 격려를 주신 분들이 떠올라 이렇게 짧은 글을 빌어 감사의 마음을 전합니다.

우선 6년 동안 항상 믿고 과제들을 맡겨주시고 많은 가르침을 주신 은수용 교수님께 깊은 감사의 말씀을 드립니다. 그리고 연구와 강의로 바쁘신 가운데에도 저의 학위 논문 심사를 맡아주시고 많은 조언을 해주시는 정성철 교수님과 박주민 교수님, 김세재 교수님 과 이성희 부사장님께 진심으로 감사 드립니다.

학위과정에서 애정과 관심을 보여주신 강희경 교수님, 유은숙 교수님, 고영상 교수님, 조문제 교수님, 현진원 교수님, 박덕배 교수님, 이영기 교수님, 윤상필 교수님 그리고 동물실험에서 많은 도움을 주신 강원석 선생님께 진심으로 되는 감사를 드립니다. 최지강, 최수길, 김영미, 강경아, 박미경, 김영미, 이혜자, 강정일 등 대학원 선배들에게도 고마운 마음을 전합니다.

그리고 한 실험실에서 동거동락을 같이 하며 물산업과제를 수행하면서 발벗고 나서서 많은 도움을 준 윤실이, 문석이, 지연이 에게도 감사의 마음을 전합니다.

6년 동안 믿고 기다리고 지지해준 신랑과 가족과 친구들에게도 진심으로 되는 감사의 마음을 전합니다. 학위과정에서 때로는 아프고 힘들어서 포기하고 싶을 때도 많았지만 그럴 때마다 저에게 힘을 주신 많은 분들 덕에 잘 이겨낼 수 있었던 것 같습니다. 모두들 언제나 건강하시고 만사형통하시길 바랍니다. 감사합니다.